Deglaciation events in part of the Manchester South 7.5'quadrangle, south-central New Hampshire

Byron D. Stone

U. S. Geological Survey

Open File Report

71-269

1971

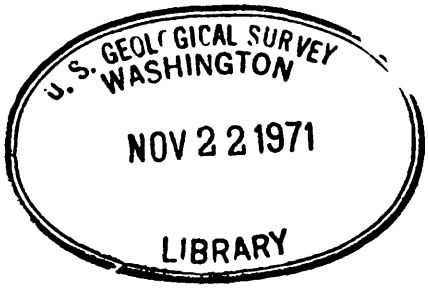

Abstract

DEGLACIATION EVENTS
IN PART OF THE
MANCHESTER SOUTH 7.5' QUADRANGLE
SOUTH-CENTRAL NEW HAMPSHIRE

by Byron Stone

The study-area lies in south-central New Hampshire, and is bordered on the west by the Merrimack River, the principal north-south drainage route of central New Hampshire.

The classical two tills of New England outcrop in the area. In a unique exposure of the sandy upper till, a loose ablation unit overlies a compact basal unit. Both upper till facies overlie a sheared section of dense, olive-gray lower till.

Outwash sequences mapped in the study-area are progressively younger to the north, indicating backwastage of the Wisconsinan ice sheet.

Primary structures in proglacial Lake Merrimack sediments include contorted bedding, buckled laminae, and folds. A large slumped section in lake sediments exhibits three distinct deformation zones, characterized by brittle, ductile, and unconsolidated deformation. Cross-cutting relationships establish four fold generations and a deformation sequence in the slumped section. Slip in each fold generation was along nearly parallel slip-lines, as deduced from analyses of fold rotation senses.

The primary and slump deformation features contrast sharply with the intense style of deformation of lake beds below till at an apparent ice readvance cut. The deduced drag fold slip-line agrees with till fabric point maxima and dip-slip on one group of thrust faults. A southerly movement of readvancing ice is inferred.

The study-area was deglaciated about 13,000 years ago, according to a proposed deglaciation model for New Hampshire. The model is based on Nye's theoretical glacier surface gradient, and evidence for active retreat of the Wisconsinan ice sheet.

PREFACE

In 1965, the New Hampshire Department of Economic Resources and Development initiated the present surficial mapping program, in cooperation with the U. S. Geological Survey. The program is designed to produce detailed surficial maps of both 7.5' and 15' scale, which will supplement the 1:250,000-scale state surficial map, published by the Goldthwaits in 1951. Mapped materials include glacial and postglacial sediments that blanket the metamorphic bedrock of the state. The first map constructed in the program is the Milford 15' quadrangle, published in 1970 by Carl Koteff, U.S.G.S., field coordinator of the program.

The author mapped much of the southeast portion of the Manchester South 7.5' quadrangle, shown in plate 1, during the summer of 1970, when he was field assistant to Mr. Koteff. Mr. Paul Banks ably assisted in the summer field work. Messrs. Graham J. Larsen and Kevin Reddy mapped deposits north of Litchfield Road and south of the Manchester airport in 1969. Their field notes and maps were of great help in the preparation of plate 1.

The author is indebted to Carl Koteff for his many suggestions in map interpretation, field procedures, and discussions of the nature of deglaciation in New England.

Many of the ideas set forth in this report are the results of informal discussions with Carl. Professor W. P. Wagner's critical review of the manuscript and comments on geologic interpretations are gratefully acknowledged. Professor R. S. Stanley encouraged the author's investigation of slump and readvance structures, and critically read the structural analyses presented in this report. Special thanks are due Mrs. Dena F. Dincauze, for her information on the Paleo-Indian site in Manchester, and Mr. Richard Bond, for his core data of the Cohas Brook muck deposits. Mr. L. R. Page, U.S.G.S., inspected the readvance site with the author, and provided stimulating comments as to the nature of deformation. Appreciation is extended to the men of the Grenier Field engineering and fire department crews for their help in cleaning the readvance cut. Mrs. L. R. Bushnell typed the final draft of this report. The author received financial support from an N.S.F. Traineeship while attending the University of Vermont, for which he is sincerely grateful.

TABLE OF CONTENTS

LIST OF FIGURES

Chapter 1

INTRODUCTION

Location

The Manchester South 7.5' quadrangle occupies an area of 53.6 square miles in south-central New Hampshire, as located in inset A, plate 1. The quadrangle lies between north latitudes 42°52'30" and 43°00'00", and west longitudes 71°22'30' and 71°30'00". The 21.8 square miles described in this report are located in the southeast two-thirds of the quadrangle, shown in plate 1. Interstate Route 93 bounds the study-area on the north, and the Merrimack River borders the area on the west. The study-area lies in Hillsborough and Rockingham counties. Much of the area is situated in the town of Londonderry; a southwest portion lies in Litchfield, and a northern portion is within the corporate limits of the city of Manchester.

Topography and Drainage

The mapped portion of the Manchester South quadrangle is characterized by a hilly bedrock upland on the east, and the wide, drift-filled Merrimack River valley

on the west. South-facing upland hillslopes exhibit a vague northeast-trending topographic grain that parallels the strike of bedrock units, shown in inset B of plate 1. Prominent hills are streamlined in a south-southeast direction. Many hills rise 200 to 300 feet above the river floodplain. The highest point in the area, over 520 feet elevation, is a hilltop one-tenth mile south of the Litchfield Road on the eastern quadrangle boundary. The lowest point, along the Merrimack River at the southern map border, falls below 100 feet elevation.

The entire Manchester South quadrangle lies within the Merrimack River drainage basin. Colby Brook and Watts Brook drain the southwest corner of the study-area, while Little Cohas Brook empties central upland runoff into the Merrimack River southwest of the airport. Cohas Brook meanders through a wide, swampy lowland south of I-93 to its entrance into Long Island Pond, artifically impounded at Goff's Falls. Merrimack River level is locally controlled by the Amoskeag Dam in north Manchester. Bedrock is exposed in the river channel during low-stage flow.

Purpose

Preliminary investigations and field mapping in 1969 revealed several exposures of contorted glacial lake sediments in the Manchester South quadrangle. It was hoped

that quantitative structural analyses of two of these exposures might shed light on the mode of deformation of the lacustrine deposits. Furthermore, by comparing the style of deformation in slumped beds with that of an apparent ice readvance section nearby, it was hoped that structural proof could be added to the stratigraphic evidence of ice readvance.

J. W. Goldthwait's classical interpretation of downwastage of a large stagnant ice sheet in New Hampshire (1938, 1951) is antithetic to Jahns' (1941) concept of backwastage of a solid-ice front. Jahns showed how outwash deposits in northeast Massachusetts differed in age and could be traced through a frontal zone of stagnant ice to the solid-ice front (1953). Successive retreatal positions of the ice front were deduced from the ice-contact heads of outwash and associated outwash sequences. Koteff (1970) mapped outwash sequences in the Milford, New Hampshire 15' quadrangle, which borders the Manchester South quadrangle on the west. Thus, it seemed that detailed surficial mapping might reveal similar outwash sequences in the Manchester South quadrangle. Coupled with precise data from the readvance cut, it was hoped that deposits in the present study-area would shed further light on Jahns' concept and the mode of deglaciation of southern New Hampshire.

Method of Investigation

Field mapping and structural analyses were completed during the summer and fall of 1970. Map units shown in

plate 1 were identified in gravel pit exposures, hand augur holes, and shovelholes which penetrated the soil c-horizon. Contacts were walked out in the field; dashed contacts in plate 1 were sketched from air photos.

Fold hinges in the slumped lake sediment exposure were measured by orienting a wooden dowel parallel to the hinge line and determining the direction and amount of plunge of the dowel with a Brunton compass. Locations of measurements were plotted on Polaroid photos of the outcrop. The schematic diagram of the outcrop, figure 5, page 33, was traced from an enlarged photo taken perpendicular to the vertical pit face.

Faults and folds were measured randomly in the readvance section, though all large thrusts were specifically included. Each measurement point was located by compass bearing and tape distance from a reference point. Location data were used to construct a schematic map of the outcrop, figure 14, page 60. The direction and amount of plunge of till pebble long axes in the readvance cut were determined by the dowel-and-compass method. Each elongate pebble encountered in the outcrop face was carefully excavated and measured in an effort to reduce operator bias.

Previous Work

C. H. Hitchcock and Warren Upham discussed the surficial deposits of the study-area in volume three of

The Geology of New Hampshire (1878). Both were concerned with the nature of deglaciation of the state, as well as local stratigraphic details. Upham described glacial and postglacial processes active in the Merrimack River valley (p. 68-103). In his classic study of New England glacial lake varves, Ernst Antevs (1922) examined Merrimack valley lake clays north of Manchester. Recent excavation has revealed rhythmically laminated clays and silts in the study-area similar to Antevs' varves.

The Goldthwaits mapped the Quaternary deposits of the Manchester South quadrangle. Their state surficial geologic map (1951) shows extensive stratified sand and silt outwash overlying lake sediments on both sides of the Merrimack River valley. The Goldthwaits make note of an ice-dammed proglacial lake in the Merrimack valley, though it is unclear where they mapped lake deposits in the present study-area.[1] The U.S.D.A. Soil Conservation Service (1953) has published a detailed map of the surficial deposits and soils of Hillsborough county.

---

[1]For several decades, workers have informally referred to the proglacial lake in the Merrimack valley as Lake Merrimack. Koteff (1970) formally cited glacial Lake Merrimack. The lake extended from Nashua, New Hampshire (inset A, plate 1) to above Franklin, New Hampshire. The nature of the Lake Merrimack drift dam at Newburyport is presently unclear (Koteff, 1971, personal communication).

Bedrock Geology

The bedrock geology of the Manchester 15' quadrangle is presented in a New Hampshire Department of Resources and Economic Development bulletin by Aluru Sriramadas (1966). Inset B of plate 1 is a bedrock map of the present study-area drawn from Sriramadas' map. Although bedrock outcrops are small and widely scattered, Sriramadas was able to differentiate five map units. The Massabesic gneiss, late Devonian (?) coarse, foliated, quartzose gneiss underlies Quaternary deposits in the northern half of the study-area. The upper member of the Silurian (?) Berwick Formation, a coarse, quartzose gray schist, is predominant in the southern portion of the area. A small outcrop of gray schist of the lower Devonian Littleton Formation lies near the southwest corner of the map, and a small folded band of binary granite is situated in the southeast corner. Only two sizable outcrops of a coarse microcline-albite pegmatite are shown on Sriramadas' map. The binary granite underlies the highest point in the study-area, indicating greater resistance to Pleistocene ice erosion than the other units. Regional strike of bedrock units is N40°E.

Accessability and Culture

Interstate 93 links Manchester, New Hampshire's largest city, with Concord to the north, and Boston, 38

miles south. Two interchanges to I-93 are located in the study-area one mile north of the airport. Three primary roads, State Route 3-A, High Range Road, and Mammoth Road provide north-south access through the study-area. Litchfield and Perimeter Roads are the two principal east-west avenues. The Boston and Maine railroad maintains two north-south freight lines in the map area. The Manchester airport is adjacent to inactivated portions of Grenier Field, a U. S. Airforce base just south of the runway complex.

The culture of the area is characteristic of creeping suburbia. Housing developments are expanding along Route 3-A near the airport and the Litchfield Road. Most inhabitants of the area work in the industrial centers in and around Manchester. Agricultural activity is limited to small fields, orchards, and private gardens. Uplands away from populated areas are covered with dense second-growth vegetation and swamps.

Significant Surficial Exposures

Active pit operations during the 1970 mapping season revealed several fresh exposures of surficial deposits along Route 3-A. Terrace sands truncate delta foreset beds at two elevations in a pit .2 mile from the southern map border, locality 1 in plate 1. The delta sediments make up the bulk of the elliptical hill encircled by lower

terrace deposits, easily seen in plate 1. This pit is hereafter referred to as the delta remnant pit. Ice-contact sandy gravel is exposed in a small pit .4 mile west of the Rockingham-Hillsborough county line, .45 mile north of the map border. This exposure is designated the Litchfield powerline pit, locality 2. Folded and faulted lake sediments crop out in an abandoned pit .45 mile south-southeast of the mouth of Little Cohas Brook. The structures in this slump pit, locality 3, are fully described in chapter 4. Primary deformation of lake beds is apparent in another abandoned pit .1 mile north of the slump pit. This exposure is termed the back-road pit, locality 4. Five-tenths mile east of the back-road pit, on the north side of Perimeter Road, till overlies distorted lake beds in an apparent ice readvance cut, locality 5. Structures in the disturbed sediments are described in chapter 5.

Two upland till quarries show significant features of till stratigraphy. Loose ablation till overlies compact basal till in a small pit north of Hall Road, .1 mile south of the Boston and Maine railroad line in North Londonderry, locality 6. These same till facies are bared in a large cut on Mammoth Road just north of the Hillsborough-Rockingham county line. Underlying the two till facies in the Mammoth Road pit is a dense olive-gray lower till. This exposure is referred to as the two-till cut, locality 7.

Chapter 2

QUATERNARY DEPOSITS

Quaternary deposits in the study-area consist of materials deposited by glacial ice or meltwater, and postglacial sediments laid down by water and wind. Proglacial lake sediments, though chronologically part of the glacial stage, are here considered non-glacial. Quaternary deposits are described below, generally from oldest to youngest.

Glacial Deposits

Lower Till. The lower till is a yellowish-brown (10YR 4-5/2-3, color code based on Munsell Soil Color Charts for naturally moist samples) to olive-brown (2.5Y 4-5/3-5) to olive-gray (5Y 4-5/2-3), hard, poorly sorted mixture of clay silt, sand, pebbles, cobbles, and few boulders. It commonly contains up to 40% silt and clay (Koteff, 1970, personal communication). A sub-horizontal joint system generally splits the till into thin platy slabs. A less well-developed sub-vertical joint set, often heavily iron-stained, is also common. Pebbles are generally rotted and friable. The brownish color is generally interpreted to be the product of extensive weathering. The lower till probably represents a pre-

Wisconsinan ice advance in New England (Pessl and Schafer, 1968; Schafer and Hartshorn, 1965), though it has been argued that the lower till is the compact basal till of the last ice sheet (Upham, 1878). The lower till has been described elsewhere in New Hampshire by Upham and Hitchcock (1878), the Goldthwaits (1951), Denny (1958), Koteff (1970), and Pessl and Koteff (1970).

Two exposures of the lower till outcrop near the top of the northwest-southeast trending hill north of I-93, just east of Wilson Road. Only a few feet of till are exposed in the abandoned pits. A ten-foot section of lower till is exposed in the two-till cut on Mammoth Road, shown in figure 1a. Blocks of unoxidized dark-gray (5Y 3.5-5/1) till have locally been sheared upwards into the olive zone, presumably by the advance of the last ice sheet (Koteff, 1971, personal communication). Both joint sets are distinct below the shear zones. The lower till is truncated sharply by overlying upper till.

Upper Till. The upper till is light-to-dark-gray (5Y 5-7/1), poorly compacted, and distinctly sandy. It contains more boulders and a smaller silt and clay fraction than the lower till. Jointing is absent. Postglacial weathering has lightly oxidized the upper three feet of till to a yellowish, or rusty color. The upper till forms an uneven, ubiquitous blanket over the bedrock uplands. The upper till in New Hampshire is described by the workers listed above.

Two upper till facies are recognized in the study-area. In the Hall Road pit, locality 6, a loose, porous upper facies rests on top of a more compact, crumbly lower zone. Low-angle shear planes are present in the lower member just below the contact. The same two facies are exposed in the two-till cut, shown in figure 1a, b, where each zone is locally ten feet thick. A representative section measured:

eolian (?) sand,	3 feet	lateral gradation ⟷	10 feet homogeneous, unsorted upper facies of upper till
sand lens	2 feet		
gravel lens	3 feet		
sand lens,	1 foot		
basal upper till	8 feet		
lower till	10 feet		

The upper facies is characterized by lenses of stratified sands and gravels which grade laterally into unsorted patches of till, probably flowtill (Hartshorn, 1958). Many of the water-laid lenses may be traced up to 100 feet in the upper facies. Note the difference in texture, and the sharp contact between the two upper till facies in figure 1b. The lower facies is interpreted to be a lodgement till, whereas the upper unit is ablation till melted from the receding Wisconsinan ice sheet.

The two-till cut may be unique in New England in that it bares thick, undisturbed sections of both upper till facies. Further, the upper till overlies a sizable exposure of sheared lower till.

Ice-Contact Stratified Drift. A six-foot section of ice-contact stratified drift is exposed under the Litchfield powerline at locality 2. Interbedded, stratified

gravel and sand lenses, up to two feet thick, are slumped internally as well as near presumed ice-contact hillslopes. Cobble-size gravel in a sandy matrix is the predominant texture, though boulders over one foot in diameter are present. Coarse-to-fine sand units are common. Lenses of diverse grain size cross-cit and truncate other lenses, and nearly all bedding is distorted. Melting of ice blocks within the deposit, in addition to wasting of the confining ice wall, deformed the bedding. Similar ice-contact gravels and sands are exposed in a kame pit just north of the Kimball Road golf course, one mile east of the Rockimgham-Hillsborough county line, .7 mile south of Litchfield Road.

Outwash Deposits. Cobble gravel grades laterally into coarse-to-fine sands in an outwash sequence that heads at the Kimball Road golf course, .8 mile from the southern map border. Pebbly, coarse sand lies in undisturbed fluvial cross-beds in a pit .5 mile south of the golf course. Coarse-to-medium sands of a small outwash sequence surround the kame just north of the golf course. Outwash cobble gravel is exposed in large pits under the Litchfield power-line locality 2. Outwash deposits in the study-area are probably less than 30 feet thick.

a.

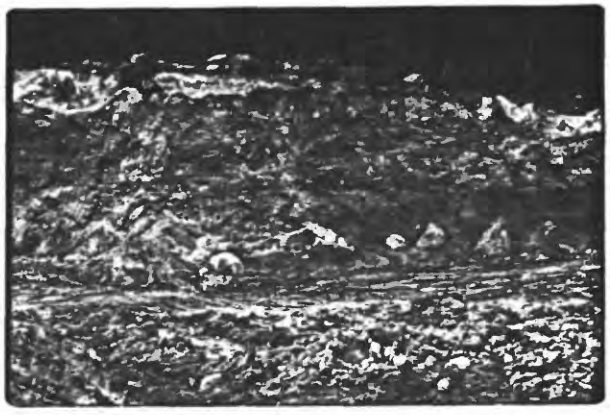

b.

Figure 1

Details of the Mammoth Road two-till cut. a. West wall of pit, exhibiting dark-olive lower till, overlain by gray lower facies and light-brown upper facies of upper till. Large boulders are about 2.5 feet diameter. b. Compact basal facies of upper till overlain by loose ablation facies. Total outcrop is about 15 feet high.

Non-glacial Deposits

Glacial Lake Merrimack Deposits. Offshore proglacial lake sediments are rhythmically laminated fine sands, silts, and clays. Laminations rarely exceed 1.5 cm in thickness; most are .5 to 1.0 cm thick. White, unoxidized fine sand grades upward into silt and clay, dark olive-gray (5Y 3-4/2) to dark grayish-brown (10Y 3/1-2). Folded and faulted laminate are shown in figures 13a and 13b, page 57. Rounded, ice-rafted pebbles are common in all exposures. Ernst Antevs (1922) assumed an annual cycle of deposition of each graded lamination, or varve. Sand was laid down in summer months when active streams carried material into the lake. Winter ice cover allowed silts and clays to settle out on the lake bottom. Antevs included several Lake Merrimack sections around Concord, New Hampshire in his investigation. Graded, offshore deposits exposed in the Merrimack valley in the present study-area are similar to Antevs' varves, and may represent a yearly deposition cycle. Primary folds and bedding convolutions, shown in figure 15, page 63, indicate instability of the clay-rich beds, as discussed briefly by Antevs (1922, pp. 72-73). Large-scale primary deformation of off-shore sediments is discussed in chapter 4.

Delta foreset beds overlying offshore laminae are

composed of sorted, medium-to-coarse sand. Foreset beds dip between 22° and 30°; direction of dip is generally toward the center of the valley. Delta sands are over 50 feet thick in pit exposures along Route 3-A. Delta foresets in the map-area are truncated by stream terrace deposits, so no topset beds are exposed. Topsets in the western third of the Manchester South quadrangle are pebbly, coarse sand, resembling outwash deposits.

Stream Terrace Deposits. Stream terrace fluvial sediments vary from sandy gravel to moderately-sorted fine sand. Terrace deposits are up to 15 feet thick in the delta remnant pit, locality 1, but they are nearly absent from the terrace surface above the slump pit section, shown in figure 4, page 30. Terrace fluvial cross-beds dip downvalley. Finer terrace sands may be confused with eolian sand in augur holes. Terrace sands are generally oxidized to a pinkish or red hue, while the eolian sands are characteristically pale yellow.

Cohas Brook Organic Sediments. Mr. Richard Bond, U.S.D.A. Soil Conservation Service, Milford, New Hampshire, cored swamp deposits in the Cohas Brook basin in 1969. The deposits are apparently organic muck mixed with silt and fine sand. No true peat was found. Depth of muck is over 30 feet in the northeast-central portion of the swamp (Bond, 1971, written communication). Core depths

to refusal indicate an abrupt deepening of the basin 200 feet north of the southern swamp boundary under the powerline reentrant. Moreover, muck depth suddenly increases near the northeast Mammoth Road swamp contact. It is assumed that the muck lies in a deep depression outlined by a steep scarp that roughly parallels the entire swamp border, shown in plate 1.

Eolian Deposits. Wind-blown sand is very well-sorted, fine-to-medium sand that commonly contains mica flecs up to 2 mm diameter. The sand is characteristically pale yellow, and maintains the same grain size in deep augur holes. Where eolian sand is over five feet thick, it is shown as dune sand in plate 1. Dune topography is discussed in the following chapter

Recent Alluvium. Recent Merrimack River floodplain deposits are generally finer grained than older stream terrace fluvial sediments. Modern floodplain alluvium is mostly white, unoxidized silt and fine sand. Abandoned channel deposits are undifferentiated in plate 1. Narrow tributary stream alluvium, shown in plate 1, is generally medium-to-coarse sand where streams cut through the delta and terrace sands. Cobbles and boulders appear along segments of streams in upland till areas.

Chapter 3

DISTRIBUTION OF QUATERNARY DEPOSITS

The distribution of glacial drift in the study-area, as mapped in plate 1, is related to the mode of deglaciation of the region. Theories of the nature of recession of the last ice sheet are discussed below. Map patterns of glacial deposits are interpreted in light of Jahn's sequence concept, the most recent hypothesis of deglaciation.

Theories of Deglaciation

Upham (in Hitchcock, 1878) pictured a downward melting ice sheet -- the surface of the ice remaining generally parallel to the underlying topography. Sediment-laden meltwaters flowed through channels in the ice to proglacial channels of deposition. J. W. Goldthwait (1938, 1951) favored downwasting of a large stagnant ice sheet. Superglacial streams carved channels at random elevations around emerging topographic highs, or nunataks. Glacial debris accumulated in the valleys around the decaying ice masses. Richard Jahns (1953) agreed with Goldthwait's early nunatak stage and initial downwastage. In contrast to earlier workers, however, Jahns showed how outwash deposits are related to underlying topography and an orderly, northward recession of an irregular solid-ice

margin.

In mapping glacial deposits in nearby northeast Massachusetts, Jahns (1941, 1953) subdivided outwash deposits into chronologic groups which he termed "sequences." Specifically, "deposits laid down by meltwaters that followed a specific outflow route constitute a single outwash sequence" (1953). Each sequence headed against the waning terminus of the Laurentide ice sheet. Meltwaters flowed in till or bedrock-floored channels around large stagnant ice blocks in front of the ice margin. Outwash streams were graded to a constant base level controlled by a bedrock threshold or glacial lake water plane. When further backwasting of the ice sheet uncovered lower outlets, meltwaters coursed along new sequence routes, or carved lower sequence levels in previous outwash deposits. According to Jahns (1953), sequence deposits grade laterally in the down-stream direction, from ice-contact eskers and kames, to kame terraces, crevasse fillings, and ice-contact plains, to outwash plains. Thus, each sequence may be traced upstream, through an ice block collapse zone, to its head at the solid-ice margin. Successive retreatal positions of the ice margin are marked by younger sequence heads. It should be noted that sequences representing retreatal positions in the region are determined by local topography and rate of backwastage, and do not represent climatically-controlled standstills (Koteff, 1970). Outwash sequences in the study-area are similar to those described by Jahns, and mapped by Koteff (1970) in the Mil-

ford, New Hampshire, quadrangle to the west. It seems that the outwash sequence theory of deglaciation is applicable to the mapped portion of the Manchester South quadrangle.

Map Distribution of Quaternary Deposits

Glacial Deposits. The lower till, up to 100 feet thick, commonly makes up the bulk of drumlins in areas to the west and south (Koteff, 1970). No morphologically distinct drumlins are present in the study-area. Thick lower till accumulations are probably limited to the flanks of bedrock hills, as at the two-till cut on Mammoth Road, locality 7. If a pre-Wisconsinan ice sheet emplaced the lower till veneer, thick sections of the till survived subsequent Wisconsinan ice erosion in the lee of bedrock highs. Lodgement upper till further cushioned the lower till from Wisconsinan ice scour.

In contrast to the patchy distribution of the lower till, upper till forms a ubiquitous, uneven cover over the uplands. Excavation at the athletic field near the eastern perimeter of the Manchester airport showed upper till below outwash deposits mapped in plate 1. It is assumed that upper till similarly underlies many other Wisconsinan glacial and postglacial deposits in the area. Well-weathered bedrock outcrops, lacking striae or grooves, indicate a long period of postglacial subaerial weathering.

The upper till cover over these outcrops was probably very thin or totally absent. Fresh, well-polished bedrock surfaces show striae and grooves where recent construction has removed the till cover.

Ice-contact deposits are conspicuously scanty in the map-area. A distinct topographic bench exists within the gravel body under the Litchfield powerline, at locality 2. The small body of gravel lying above the bench is probably a kame deposit, representing initial ice-contact deposition in stagnant ice. Gravel below the bench is the ice-contact head of an outwash sequence, discussed below. Lake sands abutting the bedrock hills southwest of Crystal Lake to Mammoth Road may be in part ice-contact. Meltwaters, damned by ice in the Cohas Brook basin, flowed west over the spillways at the airport athletic field, shown by the meltwater channel arrows in plate 1. The sand accumulated along the front of the ice, but further ice withdrawal removed the sediment source and opened more northerly drainage routes.

Outwash gravels at the Kimball Road golf course grade down-sequence into coarse sands before disappearing under the swamp near the base of the map. Gravel in the Litchfield powerline outwash sequence, locality 2, extends south to the map border. The gravel is graded to a 245 foot level controlled by a threshold in the swamp in the adjacent Nashua North quadrangle. An ice mass, one mile

wide west of the Litchfield powerline sequence, channeled meltwater flow south along the valley wall to the threshold. Subsequent stream terrace erosion of the west flank of the sequence has eraced evidence of possible lower thresholds in the ice wall. The confining ice may have been part of a stagnant ice zone, or the edge of a tongue of the solid-ice front that lay in the Merrimack valley. Outwash sediments floor two spillways at the northeast corner of the airport. A third outflow route, now deeply incised by Cohas Brook, is apparently coincident with an antecedent bedrock low. Future work north of I-93 may reveal extensive outwash deposits in the deeply carved meltwater channels indicated in plate 1.

Non-glacial Deposits. Non-collapsed Lake Merrimack delta topset-foreset contacts are exposed in pits west of the Merrimack River in the Manchester South quadrangle. These contacts represent the elevation of the lake water plane at the respective pit locales. Six elevations of the water plane, leveled from nearby bench marks, appear at their proper latitudes along the western border of the map-area in plate 1. Postglacial isostatic rebound has tilted the lake water plane upward to the north at a rate of 4.2 feet per mile in the Manchester South quadrangle. Delta sands in the study-area are graded to elevations from about 220 feet at the base of the map, to over 240 feet just south of I-93. Lake sands occupy tributary

arms of the lake north of the Kimball Road golf course, and in the Cohas Brook basin. The lake water plane was the base level for the small outwash sequence just north of the Kimball Road golf course, and the spillways at the airport athletic field. Offshore lake sediments are exposed under delta sands in pits east of Route 3-A. A small outcrop of offshore lake clays and silts is exposed along the Merrimack River bank at the base of the map.

River downcutting and lateral erosion subsequent to draining of the lake produced a nearly continuous belt of terrace sands and gravels along the east side of the Merrimack River valley. Separate terrace levels are shown by solid contacts within the light-green map-area in plate 1. Some terrace levels are less than ten feet apart vertically, though ten-foot contour lines generally follow terrace scarps, as along Route 3-A, one mile north of the southern map border. The highest terrace extends from the southern map border to I-93. The terrace trace near the airport is approximate, due to runway construction. Smaller, lower terraces are especially well developed near the Litchfield powerline. The highest terrace, and a few lower surfaces, have paired equivalents west of the river. Correlation is impossible, though, where terrace remnants are separated laterally over long distances. Only the highest terrace is extensive enough for an accurate

gradient determination, about 4.0 feet per mile.

An eolian mantle of fine sand and silt covers nearly all Quaternary deposits in the map-area. In the uplands, the wind-blown cover is generally less than one foot thick. Where eolian sand is at least five feet thick, it is shown as dune sand in plate 1. A presently active dune field, stippled in plate 1, lies under the powerline east of Route 3-A, north of Watts Brook. Relict dunes in the cleared fields just south of the Litchfield powerline appear as low, rounded east-west trending lobes. Similar rounded, hummocky dune topography overlies lake sediments south of the delta remnant pit. Vegetated dunes west of the High Range Road, .5 mile north of Litchfield Road have east-facing slip faces and horns pointing to the west. The 230-foot contour outlines one of these dunes .5 mile north of the Litchfield Road. The 320-foot hill just north of the Litchfield powerline gravels is capped with over ten feet of eolian sand. The closed depression on the north-east flank of the hill is a large blowout. The blowout floor is not swampy, as are nearby till-bounded basins. Apparently the well-sorted eolian sand drains all surface runoff from the blowout floor. Vegetated dune deposits extend north of Litchfield Road under a new housing development.

The terrace deposit-alluvium contact along the Merrimack River delimits the modern river floodplain. The

line is the high water mark of the March 1936 flood, the highest flood recorded in historic times (Green 1964, pp. 112-113). The floodplain abuts a terrace scarp or lake sediment wall along the entire map-area of the river. Tributary streams are deeply incised into delta and terrace sands, and have narrow floodplains.

Chapter 4

SLUMP PIT STRUCTURES

Offshore Lake sediments are exposed in the slump pit, locality 3, plate 1, .45 mile south-southwest of the mouth of Little Cohas Brook. The sediments are displaced along reverse faults and graben near the southern end of the pit. Interbedded sand and silt beds are folded and faulted in a slumped section at the north end of the pit. Undistorted lake beds overlie both disturbed sections, indicating that deformation occurred subaqueously shortly after deposition of the deformed sediments. The reverse faults and graben displace delta sands that overlie the slump section, and are, therefore, younger than the slump structures.

Graben

Graben and high-angle reverse faults are developed in compact, thinly bedded, fine-to-medium sands and silts at the base of the exposure, shown in figure 2a. High-angle normal and reverse fault planes are distinct, and fault traces in the pit wall are generally straight. A few faults that are continuous into upper deltaic sands are curviplanar. Most fault traces are less than five feet long. Marker beds of highly oxidized sand clearly

show the amount of apparent slip on the fault planes. Apparent dip-slips are generally less than six inches, though a displacement of 11.5 inches was measured on one fault plane. A cumulative downard displacement of 62.5 inches to the northwest was measured on 18 faults along a 15 foot-wide exposures.

A conjugate set of normal faults bounding a graben is shown on a lower-hemisphere, equal-area stereogram in figure 2b. The fault planes strike northwest-southeast. The two planes are separated by an angle of 46° in a plane, the deformation plane, that is normal to the line of intersection of the fault planes. The line of intersection of the faults is the intermediate stress axis, σ_2. The bisector of the acute arc between the planes is the axis of maximum compressive stress, σ_1. The least compressive stress axis, σ_3, lies in the deformation plane, 90° from σ_1. (Billings, 1954, pp. 95-100, 164-168; Ragan, 1968, pp. 106-112).

Figure 3 shows the angular relationships between σ_1, σ_3, observed fault planes, and planes of maximum resolved shear stress in the deformation (σ_1- σ_3) plane. The acute angle (46°) separating the two fault planes is 2θ (Hubbert, 1951, p. 364). $\phi/2$ (22°) is one-half the angle of internal friction (44°) of the faulted material. $\phi/2$ is the angular difference between planes of maximum resolved shear stress, located 45° from σ_1, and the observed

a.

b.

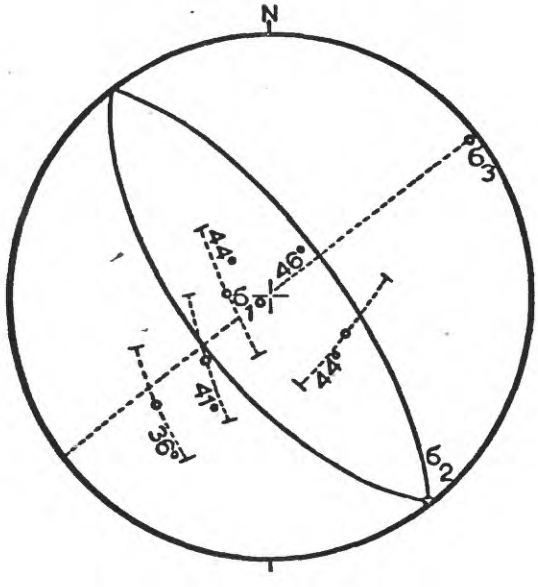

Figure 2

Reverse faults and graben in lake sediments. a. High-angle reverse faults offset lake silts and sands. Oxidized sand beds indicate apparent dip-slip movement. b. Lower-hemisphere, equal-area stereogram of two normal faults bounding a graben. Greatest principal stress, σ_1; bisects the separation arc (46°). Positions of stress axes constructed after Ragan (1968, pp. 106-112). Separation arcs and σ_1 orientations for four other conjugate fault sets are included.

fault planes. Sanford (1952, p. 48) recorded ϕ values of

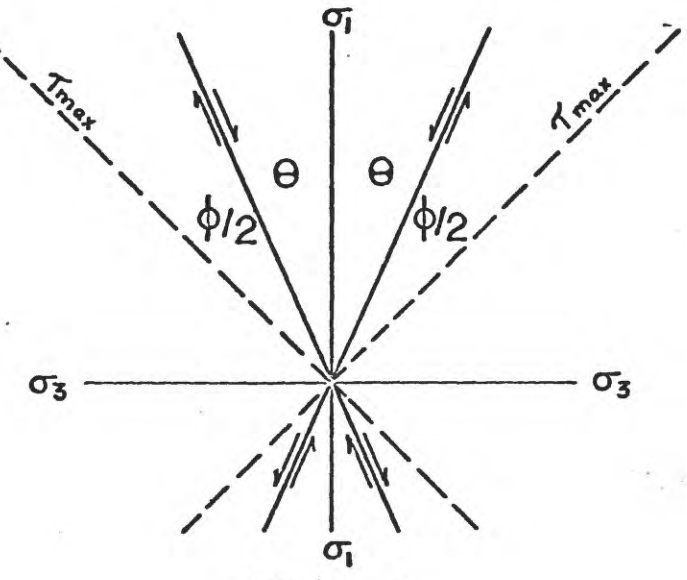

Figure 3

Figure 3. Angular relationships between principal stresses, fault planes, and planes of maximum resolved shear stress (after description of Hubbert, 1951).

about 40° for dry, mixed sand (85%) and clay (15%). ϕ values for the compact, interbedded sands and silts in the graben exposure are between 44° and 54°. Acute 2θ arcs contain-σ_1 positions for four other conjugate fault sets are included in figure 2b. Arc orientations are varied, showing random orientation of σ_2 and σ_3 in a subhorizontal plane. suggesting that σ_2 was approximately equal to σ_3. σ_1 is nearly vertical in most of the arcs. Maximum compressive stress was the vertical pull of gravity.

Graben and high-angle reverse faults are complexely interrelated in the pit exposure. Graben may be indicative of a tensile stress environment. The reverse faults may be

related to differential vertical displacement, as shown by Sanford (1959, pp. 43-48), and do not necessarily reflect principal horizontal compression. The complex fault relationships were not studied in this report. The nature and history of deformation remain unclear.

Slumped Section

Slump structures are displayed in a profile section cut nearly perpendicular to the strike of thrust faults and fold hinges. The slumped section, shown in figure 4, is about 17 feet wide, and extends upward to undisturbed silt beds truncated by a stream terrace surface. The section appears in figures 4 and 5 as it was exposed in the summer and fall of 1970. Figure 5 is a tracing of an enlarged photo of the outcrop. About 90% of the total exposure is shown, the effective undistorted width of the figure being determined by curvature of the outcrop face and camera lense distortion. Fault plane and bedding plane extensions through talus-covered portions of the diagram are included. Lines perpendicular to bedding, used to define the total shortened interval, are also shown. A reference grid system is included in figure 5. Thick sand units are stippled.

Stratigraphy. The deformed beds were measured and described in November 1970. The units are numbered sequentially from the top, and unit numbers are keyed to numbers on the right side of figure 5.

Figure 4

The slump pit section. Note zone of oxidation within the deformed section. Also note lack of stream terrace deposits at top of exposure. Total deformed section is about eight feet thick.

Unit Number	Description	Undisturbed Thickness
1	Light-gray silt containing about 20% clay. Rhythmical laminations are 1/8-inch thick. Sand lenses are highly oxidized and up to ten inches thick. An eight-inch laminated silt unit, 15 inches from the base of the unit, shows highly contorted laminae in primary load folds. The contorted silt unit can be traced 30 feet laterally. The entire eight-foot unit is cut by subvertical joints.	8'
2	Light-brown, poorly sorted, medium sand in a silty matrix. Pebbles 1 cm long are common; largest pebbles are 2 cm long. Layers of underlying laminated silt unit are subhorizontal and are up to five feet long and six inches thick. Orange oxidation stain extends $\frac{1}{4}$-inch into silt units. Heavy accumulation of black iron stain along all sand-silt contacts. No bedding or joints are present.	1'
3	Light-gray, finely laminated silt.	3.5"
4	Poorly sorted sand with silt-bed fragments, similar to unit 2. Nine-foot long unit is lens-shaped.	10"
5	Light-gray, finely laminated silt. Unit contains oxidized and unoxidized sand laminae up to $\frac{1}{4}$-inch thick.	3"
6	Fine-to-coarse, poorly sorted sand. Unit is highly oxidized dark-brown to black.	.5"
7	Light-gray, finely laminated silt. Fine-to-medium unoxidized sand laminae are 1/8-inch thick. A $\frac{1}{4}$-inch oxidation band lies along upper and lower contacts.	3"

P. 33 IS BIG PLATE

8	Bright orange, fine-to-coarse sand. Unit thickens to ten inches in section C-3. Iron-stained zone is 1.5 inches thick along top contact.	.75"
9	Light-gray laminated silt. Unit is folded into overlying sand. Oxidation band at top contact is ½-inch thick.	2"
10	Dark-orange-to-black, poorly sorted sand. Silty matrix contains about 10% granules. Unit is well-cemented by iron-stain. Unit is relatively unoxidized to the right of the fold limb in section E-3.	1"
11	Three gray silt beds, ¼-inch thick, in highly oxidized sand. Sand is poorly sorted. Silt units show some local thickening in section E-3. Unit relatively unoxidized to the right of section E-3.	4"
12	Lightly oxidized, poorly sorted sand.	1.5"
13	Two light-gray silt beds, ½-inch thick, in lightly oxidized, poorly sorted sand.	2"
14	Gray, lightly oxidized sand.	4"
15	Gray silt laminae in lightly oxidized sand.	2"
16	Gray,lightly oxidized sand.	6"
17	Gray silt bed.	.5"
18	Gray, lightly oxidized sand.	3.5"

Deformation Zones. Three stylistically distinct deformation zones are recognized in figure 5. Units in the zones responded to lateral compression during slump movement by different modes of deformation. The sand and thin silt layers below unit 10 were shortened principally

by brittle failure in low-angle thrusts. Units 10 through 5 were compressed chiefly through flexural-flow folding and flowage in the less-viscous sand layers. Unconsolidated flowage in unit 5 took place at the sediment-water interface subsequent to the slump movement below unit 5. Following a brief sedimentation interval, material in unit 2 flowed at the sediment-water fringe. Flowage in units 4 and 2 acted to fill the slumped lake-bottom concavity above unit 5. The three deformation zones are hereafter referred to as the brittle, folded, and flowage zones, respectively.

Nature of Deformation. Silt beds in the brittle zone maintain a continuous thickness across the entire exposure. More ductile interbedded sands also retain their pre-deformation thickness. A measured shortening of 44% in units 15, 13 and 11, though a minimum, is seemingly a close estimate of total shortening in the slumped section. Where competent silts are buckled, however, chevron folds are predominant. Chevron folds are well preserved in sections G-4, and H-4. Silt layers exhibit curved hinges either along, or just above their intersections with thrust fault planes, as in sections D-5 and D-6. The silt is usually smeared down the short fold limb, along the fault plane. At least 44% shortening was accomplished in the brittle zone by faulting along initially developed short fold limbs.

Units in the folded zone show a progressive lessen-

ing of apparent shortening upward through unit 5. Sand unit 10 exhibits a shortening of 37%; overlying silt unit 9 has been compressed 33%. Heavily oxidized and iron-cemented sand unit 8 has been shortened only 31%, but thickens from .75-inch to ten inches in sections C-3 and C-4. This unit shows poorly preserved bedding which has been folded parallel to the unit boundaries. All traces of bedding are lost in the center of the sand layer in sections B-3 and C-3, where displacement was greatest. A 1/8-inch unoxidized sand layer in silt unit 7 can be traced parallel to the distinctive, slightly thicker oxidized sand layer 6 in figure 6, page 39. Both sands were deformed similarly, though bed thickness and viscosity differences caused minor variation in resultant fold geometry. Sand layer 6 is apparently shortened only 24%, but thickening is pronounced in sections B-3, C-3, and D-3. Folded zone units took up compressive stress by internal ductile flow. Unconsolidated beds near the top of the zone thickened the most (and show the least amount of apparent shortening) because cohesive strength was low. Units at the base of the zone retained some competency due to the confining lithostatic pressure. Apparent shortening near the base of the folded zone (37%) approaches the shortening value for the underlying brittle zone (44%).

Internal structures in both flowage zones consist

only of subhorizontal bedding, parallel to the lower contacts, near the bases of the zones. Silt-bed fragments, incorporated in the highly contorted silty sand matrix, are balled-up and buckled. Silt-bed stringers are shown in sections B-3, C-3, B-2, and D-2. Slip-line orientations deduced from these folded silt-bed fragments, discussed in a following section, show that slip in the flowage zone was controlled by the shape of the slump depression above unit 5. Unit 4 flow occurred at the sediment-water interface after slump movement below unit 5. Even after a normal sedimentation interval, represented by unit 3 which dips a maximum of 2° in the present outcrop, the lake bottom gradient around the slump concavity was large enough to promote flow of unit 2.

Sands in the brittle zone, though similar to overlying sands in the folded zone, behaved in a brittle fashion when they faulted in response to lateral compression. Sands above silt unit 11 are highly oxidized, whereas sand units below silt unit 11 are relatively unoxidized. The silt unit has apparently acted as a seal to groundwater movement through the slumped section in postglacial times. It is proposed that this same process occurred subaqueously at the time of deformation. Pore water was trapped below silt unit 11 during deposition of units 10-5. Hydrostatic pore-water pressure increased in the lower sands, due to

the added lithostatic pressure. Hubbert and Rubey (1959, pp. 132-134) showed that increased internal pore pressure reduces the normal stress acting across planes of potential shear. J. Handin, et. al. (1963) emphasized that pore pressure reduces the values of the normal stresses by equal increments, without affecting the angle of internal friction (ϕ). Handin's experimental results showed increased pore pressure diminishes the strength and ductility of the porous material. The increase in pore pressure in the sands of the brittle zone may have approached the lithostatic pressure acting on the sands. Thus, the normal stress acting on the plane of slip was reduced to a very low value, and failure occurred. Furthermore, it is suggested that pore pressure in the lower sands remained abnormally high during slump movement. The high pore pressure helped the sand units bouy up the thrusted sections.

Folded-zone sand units 8 and 10 lay under about 7.5 inches and ten inches of sediment, respectively, at the time of deformation. Compaction so near the sediment-water interface was low, and sand unit flowage occurred along fault planes. The resulting structures in sections B-3, B-4, D-3, D-4, and E-3 appear falsely as folds with splayed hinge zones. Internal flow and fattening also acted along silt unit 9 in section C-4. The contact of sand unit 8 with sandwiching silts 7 and 9 displays a corrugated surface, indicative of contacts between materials of relatively

high ductility contrasts (Ramsay, 1967, p. 382). Contacts in the brittle zone, by comparison, are curviplanar and are not corrugated. Increased pore-water pressure in the brittle zone reduced ductility of the porous sand units.

Fold Generations and Deformation Sequence. Two generations of folds show opposite rotation shear senses and exhibit a cross-cutting relationship in the brittle and folded zones. Large and small-scale folds, appearing with a counterclockwise rotation sense in figure 5, are the oldest slump structures in the outcrop. These are designated first order, f_1, folds. Low-angle thrusts in the brittle zone are also products of a counterclockwise shear couple. The fault planes are parallel to f_1 fold axes, and are of the same deformation age. The thrusts are designated F_1 faults. F_1 movement developed in response to lateral compression that displaced upper layers to the left (northwest) over lower layers.

A clockwise sense of rotation is obvious in small folds in sections B-3, C-3, and E-3, and in figure 6, an enlarged portion of section C-3, C-4, D-3 and D-4 of figure 5. Slipline analysis, discussed in the following section, illustrates that f_2 movement was parallel to f_1 movement, but in the opposite direction. Fold generations f_3 and f_4 are assigned to the contorted silt-bed fragments in flowage units 4 and 2, respectively. F_3 movement followed f_1 and

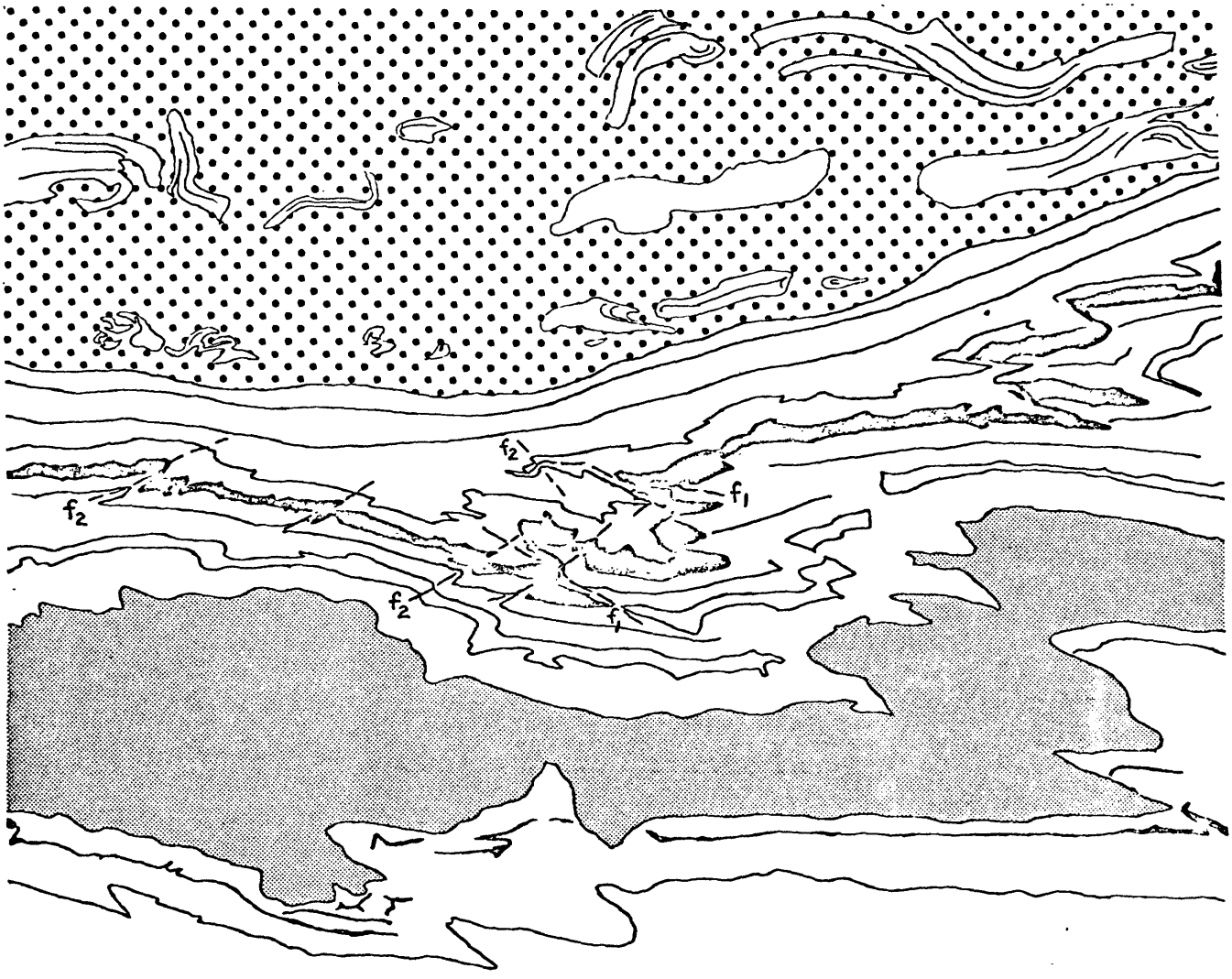

Figure 6

Cross-cutting relationships of f_1 and f_2 folds. Older, counterclockwise f_1 fold limbs and axial planes (dashed lines) are cut by clockwise f_2 folds. Note small counterclockwise f_2 fold in center of diagram. Diagram is enlarged from sections C-3, C-4, D-3, and D-4 of figure 5, page 33.

f_2 slumping, and f_4 flowage occurred after emplacement of the f flowage unit.

Slip-line Analysis. The fold slip-line is the direction of movement of one layer or body of material past another (Hansen, 1965, p. 392). In asymetrical folds, such as the folds in the slump outcrop, it is the direction of maximum movement or translation of the long fold limb over the short fold limb. Hansen (Hansen et. al., 1961) discovered in folds in glacial sediments, and in a tundra landslide (1965) that the slip-line is contained in the separation arc, the arc defined by the angle which separates groups of fold axes with different rotational senses. Hansen (1965, p. 392) showed that the slip- line coincided with the bisector of the separation arc. In the present study, this bisector is assumed to parallel the slip direction. This assumption is more valid in cases with small separation arcs than larger ones. Scott (1969) analyzed experimentally produced drag folds and proved an earlier assumption (Hansen, 1965) that fold axial planes share a common zone axis. The pole to the slip plane and the axial plane zone axis define the deformation plane for the total fold fabric. The line of intersection of the slip plane and the deformation plane is the slip-line, shown in figure 7. In Hansen's and Scott's work, it was shown that σ_2, the intermediate principal stress is perpendicular to the slip direction and parallel to

the slip surface. σ_1 and σ_3, the maximum and minimum principal stresses, respectively, are oriented in the deformation plane. σ_1 is inclined from the slip-line by an angle θ, shown in figure 7. σ_1 and σ_3 may rotate about σ_2 during deformation, but such rotation does not alter the orientation of the deduced slip-line (Hansen, 1965, pp. 394-395).

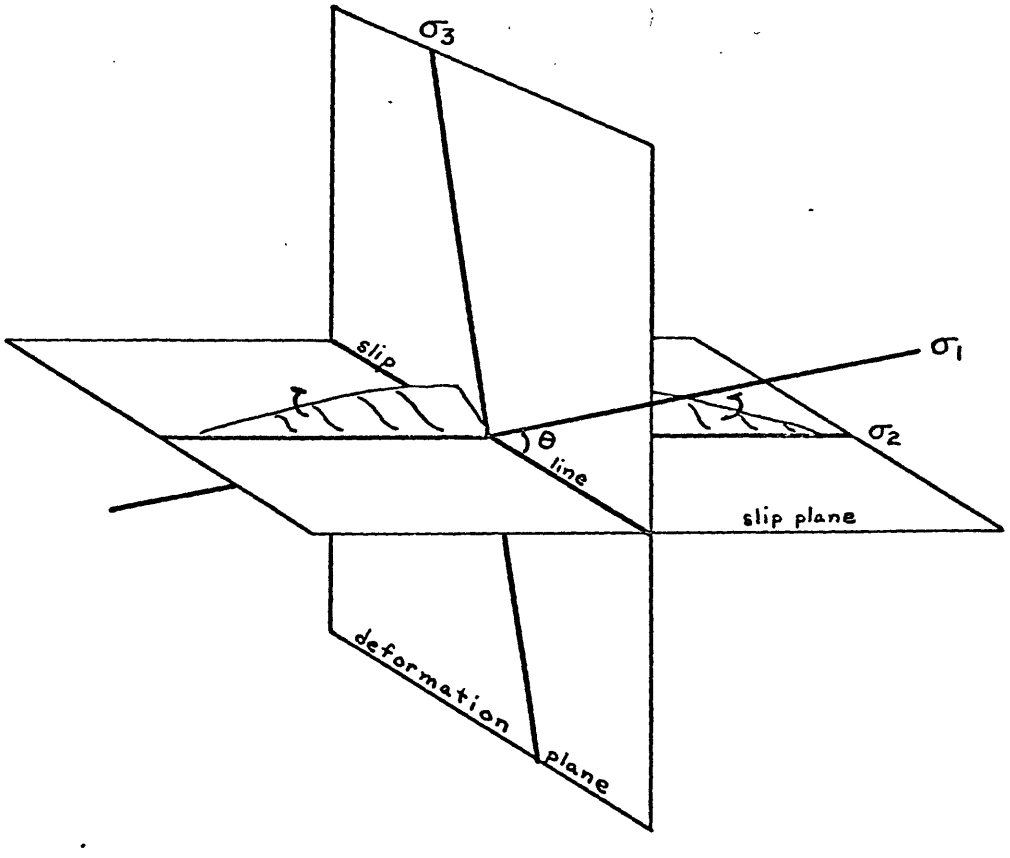

Figure 7

Geometry of slip-line analysis. Curved fold hinge lies in slip plane, which approximately parallels original layering. Line of intersection of the deformation plane and slip plane is slip-line. Note that rotation sense of the fold is opposite on either side of the slip-line.

Slip-line orientations of f_1, f_2, f_3, and f_4 folds are shown on lower-hemisphere, equal-area stereo projections in figure 8a, b, c, and d. The number of hinge measurements for each slip-line determination, and the orientation of each slip-line and slip-plane are included in the diagrams. Diagrams 8e, f, g and h are projections of the poles to the axial planes of each fold generation. Planes shown as solid great circles in figures 8e and 8g limit the range of great circles that could be used to describe the axial plane data. Dashed great circles, drawn through the pole to the respective slip plane and limiting zone axes (poles to the solid great circles), show the range of orientation of deduced deformation planes. Slip-line orientations deduced from zone axis data lie at the point of intersection of the deformation plane (dashed great circle) and the separation arc in the slip plane. Observations of the diagrams are summarized below:

f_1 folds show no anomalous rotation senses in figure 8a. Fold hinge orientations are grouped in an 89° arc in both the northeast and southwest quadrants. The bisector of the separation arc (slip-line) plunges S54°E at 30° and indicates movement of upper beds to the northwest over lower beds. The slip-line deduced from the separation arc lies within the range of slip-lines limited by the zone axis deformation plane data shown in figure 8e.

f_2 fold hinge orientations in figure 8b lie in a 72° arc in the northern quadrant, and a 93° arc in the southern quadrant. There are no anomalous rotation senses. The deduced slip-line plunges S64°E at 23°, implying that upper beds moved southeastward over lower beds along a line nearly parallel to the f_1 slip direction, but in the opposite direction. The few poles to axial planes shown in figure 8f are too tightly clustered to be used for slip-line analysis.

f_3 fold hinges, shown in figure 8c, include 16 hinges with undetermined rotation senses. The separation arc defined by fold axes where shear sense was positively identified is 86°. The three hinges of unknown rotation sense lying within the arc may be truly symmetrical, due to a combined sense of rotation (Stanley, 1970, personal communication). They may, however, belong to the counter-clockwise group, thereby defining a separation arc of 60° and a more southerly slip-line. Movement in the f_3 flow-age unit was northwestward, parallel to f_1 slip. Zone. axis slip-line orientations, inferred from figure 8g, are considerably south of the separation arc bisector. The few data in figure 8g may have yielded incorrect deformation plant orientations.

f_4 folds show the widest scatter of hinge-line orientations of all fold generations. Four anomalous shear senses appear in figure 8d. The small separation arc is

anchored by a clockwise fold in the southeastern quadrant. The arc is defined to the north by the last counterclockwise fold axis in the northwestern quadrant, selected after consideration of the arrangement of axes of unknown rotation. Figure 8d shows 12 out of 15 unknowns grouped well behind the separation arc. The deduced slip direction was to the northwest, approximately parallel to f_1 and f_3 slip-lines. Poles to axial planes are widely scattered in figure 8h, and are not used for slip-line analysis.

Deformation Plane. Contoured poles to eight brittle zone thrusts are shown in figure 90. Fault plane pole maxima contain the poles to f_1 and f_2 slip planes, indicating the slip planes are coincident with the fault planes. Apparently, f_1 and f_2 folds developed as drag folds along planes of high shear stress. The poles to deduced slip planes, and deduced f_1 and f_2 slip-lines define the slumped section deformation plane, shown in figure 9b. The deformation plane great circle was drawn between the f_1 and f_2 slip-line orientations, and between the f_1 and f_2 slip plane poles. The strike of the nearly vertical deduced deformation plane is approximately parallel to the strike of the outcrop face, N46°W.

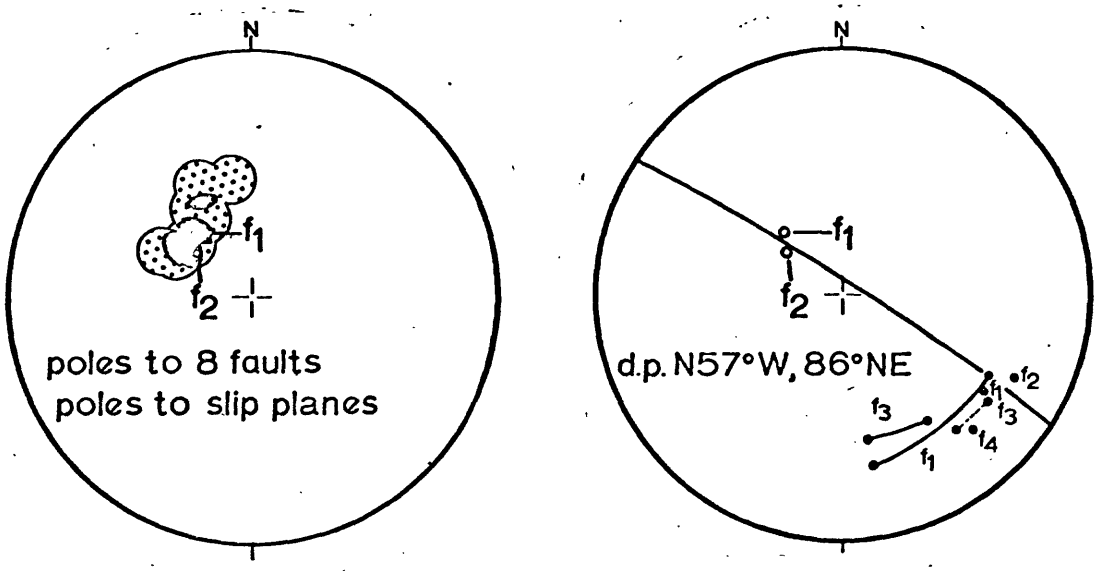

Figure 9

Deduced deformation plane of slumped section. a. Contoured poles to eight faults. Contour intervals 12.5% and 37.5%. f_1 and f_2 poles to slip planes included. b. Deformation plane (d.p.) constructed between f_1 and f_2 slip-lines and poles to f_1 and f_2 slip planes.

Stress Field Analysis. M. K. Hubbert (1951, pp. 367-371) discussed the positions of maximum and minimum compressive stresses in a model squeeze box, where the deformation plane was parallel to the glass side of the box. His stress field analysis is particularly applicable to the slumped exposure because the deformation plane

of the slumped section is approximately parallel to the outcrop face. Figure 10 is adapted from Hubbert's original diagram. Stress trajectories, lines tangent at every point to a given principal stress, are drawn for σ_1 and σ_3, maximum and minimum principal stress axes, respectively. The σ_2 trajectory is normal to the plane of the diagram, the deformationplane. Lithostatic pressure, σ_z, increases with depth in the block, and is represented by the small horizontal tensors at either end of the block. The horizontal normal stress, σ_x, increases from left (σ_{x2}) to

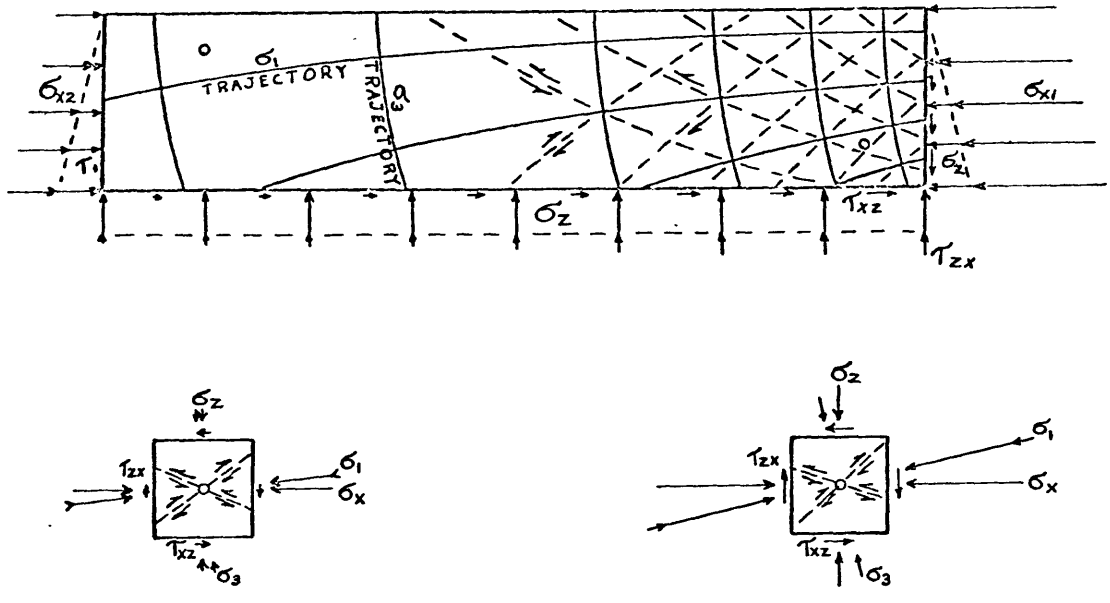

Figure 10

Stress field for thrust faults (after Hubbert, 1951, p. 370). σ_1 and σ_2 stress trajectories shown as solid lines. Planes of failure shown as dashed lines. Stress-squares below block show all stresses acting on corresponding points in block.

right (σ_{x1}), where movement is greatest at the right end of the block. σ_x also increases with depth by the incre-

ment of increased σ_z. Shear stresses τ_{xz} and τ_{zx}, forming in response to movement, increase from left to right, and in the downward direction. Thus, horizontal normal stress, σ_x, and shear stresses, τ_{xz} and τ_{zx}, are directly proportional to the intensity of deformation. Potential shear (thrust) planes, shown as dashed lines in figure 10, are drawn at angles (θ) of 30° from the σ_1 trajectory.

Hubbert (p. 369) shows that the sum of forces acting on the block in the horizontal (x) direction is zero, according to the equation for dynamic equilibrium

$$F_x = \int_0^{z1} (\sigma_{x1} - \sigma_{x2})dz - \int_{x1}^{x2} \tau_{xz}dz = 0$$

where the quantity $\int_0^{z1}(\sigma_{x1} - \sigma_{x2})dz$ is equal to the mass of the block and the component of its acceleration in the x-direction, and $\int_{x1}^{x2}\tau_{xz}dx$ is the shear stress acting along the length of the block. Diagrammatically, the state of stress acting on one point in the block may be represented by a two-dimensional stress-square, shown below the block in figure 10. The point of analysis in the center of the square corresponds to the point circled in the block. The positions of the principal stresses σ_1 and σ_3, are functions of the relative values of σ_x, σ_z, and shear stresses τ_{xz} and τ_{zx}. Shear stresses are balanced around the square so that there is no resultant rotation of the square; i.e., the square is in dynamic equilibrium. Note that the shear stress components for the upper left point are small.

Lithostatic pressure, σ_z, near the top of the block is small. Therefore, the position of σ_1 is only slightly rotated from the horizontal. By comparison, shear stresses τ_{xz} and τ_{zx}, acting on the point in the lower right corner are large; σ_z is also increased. The σ_1 trajectory is rotated toward the σ_z axis through a larger angle than in the upper left example. Thus, the σ_1 trajectory plunges greatest in the lower right corner where τ_{xz} and τ_{zx}, and σ_z values are highest.

Figure 11 is a proposed stress field for the slumped section, drawn in the plane of the outcrop which nearly parallels the deduced deformation plane. Stress trajectories were constructed at angles (θ) of 25° from the observed thrust faults, assuming a ϕ value of about 40° for the sand-silt units. Normal stresses σ_x and σ_z appear slightly rotated through an angle α from the horizontal and vertical, respectively. It is suggested that rotation took place on a hypothetical basal slip plane, shown below the talus cover in figure 11. Hydrostatic pore-water pressure is represented by the stress crosses at the left side of the section. Silt unit 11 is represented by the dotted line. Stress-squares below the section show an increase with depth of σ_z, σ_x, shear stresses, τ_{xz} and τ_{zx}, and pore-water pressure, p. It is proposed that the downward increase of normal stress σ_z was offset by abnormally high pore pressure below silt unit 11. Pore pressure also reduced

normal stress σ_x. Normal stresses acting on planes of shear were reduced to very low values during slump movement. The relative values of σ_x, σ_z, τ_{xz}, and τ_{zx} remained approximately constant throughout the brittle zone, possibly due to differential increase in pore pressure below lower silt units, or variations in σ_x through the section. The principal stress trajectories are shown as being nearly straight below silt unit 11 where observed

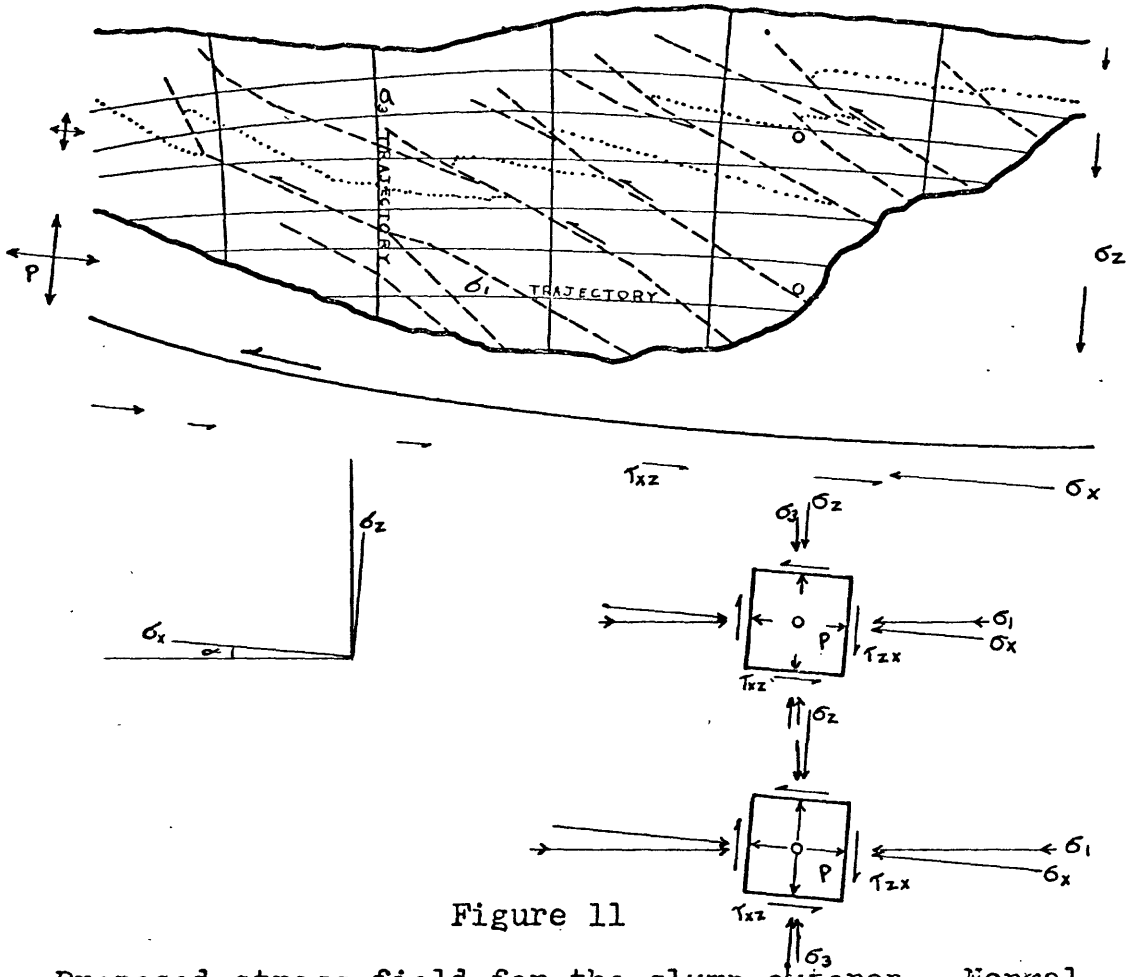

Figure 11

Proposed stress field for the slump outcrop. Normal stresses are rotated from the horizontal and vertical through angle α. Pore pressure represented by stress crosses, p. Stress-squares correspond to circled points in section.

fault traces are straight and subparallel. Fault traces and stress trajectories are curved above silt unit 11, as in Hubbert's model stress field.

Slump Pit Deformation History. Glacial meltwaters deposited alternating sand and silt units on the floor of Lake Merrimack in front of prograding delta sands. Water depth above the slumped section was about 80 feet prior to deformation, based on the elevations of the pit and the lake water plane at the latitude of the pit. Porewater pressure built up in the sands of the brittle zone during sedimentation of units 10-5. The increased internal pore pressure reduced normal stresses acting on a basal shear plane. Slip occurred, with movement to the northwest, parallel to the f_1 slip-line. Pore pressure below silt unit 11 remained abnormally high during development of the overthrusts, along which f_1 drag folds developed. A slight back-slip occurred as the f_1 movement subsided. The reverse slip followed the f_2 slip-line, and f_2 folds offset f_1 fold hinges in the folded zone. A brief period of sedimentation followed before the f_3 flowage unit was emplaced in the slump concavity above unit 5. Similarly, materials in the f_4 unit flowed into the remaining depression subsequent to normal sedimentation of unit 3. More offshore sediments were laid down on top of the slumped section before deltaic sands, advancing from the east,

buried the section. Further slumping in lake sediments may have led to deformation along high-angle reverse faults, and the development of the graben.

Chapter 5

READVANCE CUT

Compact upper till is sandwiched between lake sediments in a small bulldozer cut on the north side of Perimeter Road at locality 6. Lake sediments are severely distorted below the till, implying deformation by the weight of readvancing ice. As shown in plate 1, the lake sediment outcrop extends .5 mile east along the stream valley wall to the Merrimack River floodplain. There, rhythmically laminated lake deposits interfinger with delta sands at the back-road pit, locality 5. The sand beds thicken upward until only sandy delta foresets are exposed near the top of the pit. The same stratigraphic relationships are exposed in the slump pit, locality 4.

Readvance Cut Stratigraphy

Figure 12 shows details of the readvance cut, freshly cleaned by a front-end loader. The overlay includes contacts between four stratigraphic units, and fault traces. Stratigraphic units are described below, and unit numbers are keyed to numbers on the right side of figure 12.

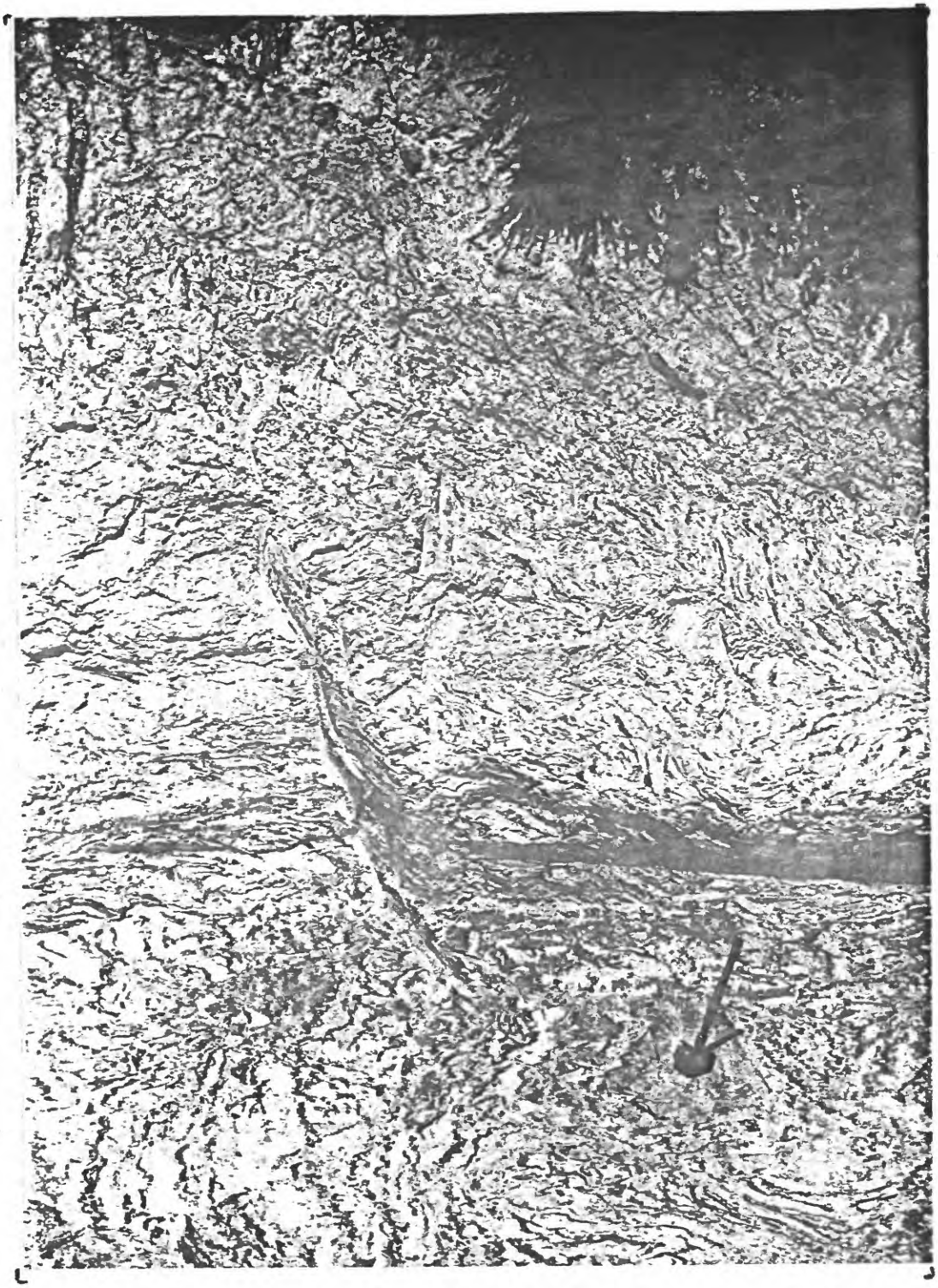

Figure 12. Details of the readvance cut. Overlay shows outline of pit floor, contacts between units described in text, bedding and fault traces. Entrenching tool handle is 20 inches long for scale. Compare with figure 14, page 60.

Unit Number	Description	Maximum Thickness
1	Thinly bedded, fine-to-coarse sand. The sand contains very few silty beds, and is lightly oxidized. Small primary deformation structures, such as minor thrusts, folds, and warped bedding, are present near the base of the sands. The structures are similarto primary structures at the slump pit and back-road pit. Unit 1 is not shown in figure 12.	8'
2	Rounded cobbles and boulders. Cobbles and boulders lie in a horizontal line below a gradational contact with the overlying lake sands. Boulders are up to two feet in diameter. There is a sharp contact at the base of the boulder zone with underlying till. This contact is shown along the top of the overlay of figure 12.	2'
3	Compact, sandy upper till, gradational downward into dense, clayey till. Maximum till thickness is shown on the right side of figure 12. The till is similar to the basal upper till of the Mammoth Road two-till cut, shown in figure 1b, page 12. A narrowsand dike lies at the base of the till near the right side of figure 12. Subvertical joints are developed near the dike. The contact of the till with the underlying mixed unit is is gradational and indistinct.	5'
4	Mixed zone of lake clays and silts, and sandy till. Discrete pices of underlying lake sediments are scarce. The few fault planes are poorly developed and difficult to trace. The contact with the lower lake sediments, shown in figure 12, cuts diagonally across the outcrop from upper left to lower right.	1'
5	Offshore laminated lake clays, silts, and fine sands. Rhythmic laminae are graded and may be varves representing yearly cycles of deposition. Faulted and folded laminae are shown in figure 13, page 57 The offshore sediments contain many pebbles, presumably melted from icebergs. Inclusions	12'

of unsorted, clayey till, up to two feet long, are scattered throughout the zone. The sediments are highly contorted and faulted, principally by low-angle thrusts.

Structural Analysis

Figure 14 is a map of the readvance pit floor and excavated faces shown in figure 12. Shown on the map are measured structural elements in the offshore sediments below the till. Traces of major fault planes in the pit face are included so that the map may be compared with the overlay of figure 12.

Faults. Fault plane traces vary from less than one inch to over ten feet long. Fault planes are commonly iron-stained. Some fault planes are filled with ashen-white, very fine sand. Faults offset marker units in only a few cases. Figure 13a shows a small reverse fault that offsets graded laminae. The offset dike, shown in figure 12, indicates the relative direction of slip on a large thrust fault. The sense of drag along fault planes was used for most slip determinations shown in figure 14. Fault planes are difficult to identify unless they strike at a high angle to the pit face. The limited exposure thus restricted structural analysis and interpretation. Nevertheless, three widely divergent groups of faults are recognized. Faults in each group are related by sense of movement, similarity of strike and dip, and style of de-

a.

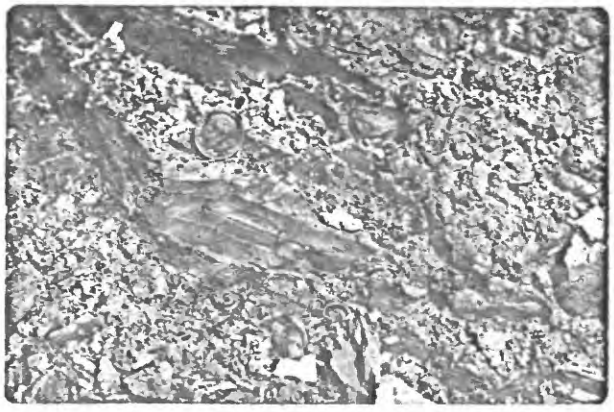

b.

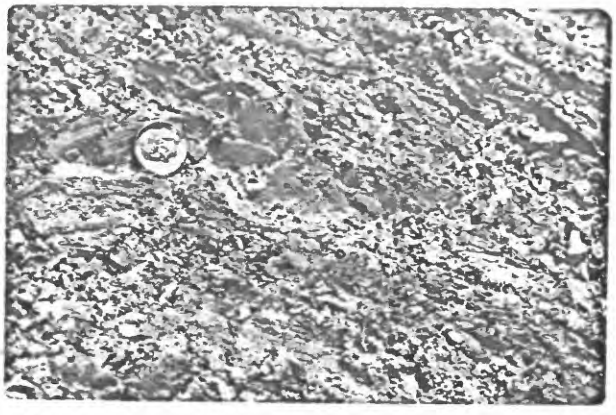

Figure 13

Faulted and folded lake sediments at the readvance cut. a. Reverse fault. b. Drag fold.

velopment, including apparent amount of slip, length of fault trace, and character of drag. Cross-cutting relationships establish a deformation order between some elements of the groups. Each fault group is described below, beginning with the youngest.

North-South Thrusts. Stereogram a of figure 14 shows seven north-south trending thrusts that dip less than 45° to the east. The dashed line connects poles to the same fault measured in two locations. Strike direction varies 77°. Fault planes are distinct and generally over one foot long. Fault traces in the north pit face, up to ten feet long, are shown in figure 12 and diagrammatically in figure 14. Four long fault traces indicate imbricate thrusting in the north pit wall above the three-foot contour. Two thrusts of this group displace the sand dike in the upper left corner of figure 12. Apparent dip-slip movement shows the upper plate moved northwest over the footwall. It is believed that dip-slip is the major slip component of the thrusts. The large arrow on the east side of the diagram indicates a slip-line orientation compatible with dip direction of most of the faults. The smaller arrows define a possible range of dip-slip directions. The variation in the strike of the same thrust measured in two locations indicates that the position of the maximum principal stress varied

P. 60 IS BIG PLATE

through the deformed zone.

Tension Features. Eight normal faults and two sand dikes, products of tensile stress, are plotted in stereogram b of figure 14. Some elements of this group may be extension features, related to horizontal compression deduced from the thrusts. Faults are small, with traces being only inches long. Dikes are over one foot long. Strike and dip of the features vary considerably, though six of the faults dip at angles greater than 45°. Tension elements are found from floor level to over ten feet above the floor. One of the sand dikes lies within the till unit. Normal faults cut the east limb of the large plunging syncline exposed in the pit floor. The age relationship between the tension group and the east-west thrusts, discussed below, is unclear.

East-West Thrusts. Stereogram c shows ten east-west trending thrusts that have an average dip of 38° north-northwest. The thrust traces are from four feet long, to less than two inches. Five thrusts of this group are located in the west pit face, from four feet to over six feet above the floor. Three members of the group lie in the pit floor, one at the western end of the north pit face, and two near the southeast corner of the floor. Two east-west thrusts cut the syncline in the pit floor. The large arrow at the north side of the diagram corresponds to dip-slip direction on a majority of the thrusts.

Smaller arrows define a possible range of dip-slip directions on the thrusts. The age of the high-angle reverse fault that offsets a prominent east-west thrust in the west pit wall is unknown.

Folds. The largest single structure in the lake sediments is the northwest-plunging syncline traced in the pit floor and in the lower north wall. Although faulting has eradicated the syncline trace in the north wall above the four-foot contour, the structure remains intact below that level. Note in figures 12 and 14 that no major thrusts penetrate the syncline below the three-foot level. A large till block lies within the fold in the bottom of the pit.

Hingelines of small drag folds, found only near the bottom of the pit, are plotted in stereogram d. One of the folds is shown in figure 13a. Rotational senses for seven out of the nine folds are shown. All folds had less than a one inch wave length, and amplitudes less than one inch. Note that no anomalous rotation senses appear on the diagram. The deduced slip-direction indicates southerly movement of upper beds over lower beds.

Till Fabric. Two 50-stone till fabrics are plotted on stereograms, bordered by rose diagrams summetric about the east-west axis, in figure 14. A composite of the two fabrics is shown in the slightly enlarged fabric diagram. The fabricswere measured in the till unit above the dis-

turbed lake sediments. The strong north-northeast point maxima in all the stereo plots are emphasized in the rose diagrams. It is assumed that the point maxima are parallel to the direction of ice movement. The transverse northwest-southeast allignment is fairly well developed in all diagrams. Because the till is apparently lodgement till, the transverse stones may have been oriented by prolonged flow in the ice where the long axes were alligned normal to shear and movement directions (Glen, Donner, and West, 1957). Holmes (1941) suggested that at least 100 stones be included in each fabric diagram. Note that each 50-stone fabric shows the major orientation maxima that the 100-stone fabric exhibits. The 50-stone fabrics would imply the same interpretation as the 100-stone fabric.

Style of Deformation. The intense style of deformation of the lake sediments below the till contrasts sharply with primary deformation structures in the back-road pit and in the slump pit. Figure 15 shows primary folding of a sand bed, exposed in lake sediments at the back-road pit. The entire block of offshore sediments containing the folded bed was apparently rotated in a large-scale slump movement, because beds dip over 15°, and strike orientation changes radically in a few feet of outcrop. The displaced offshore beds contain no thrusts or tension features like those in the readvance cut. Lake-

floor slump deformation is considered an unlikely alternative explanation for the deformation at the readvance cut.

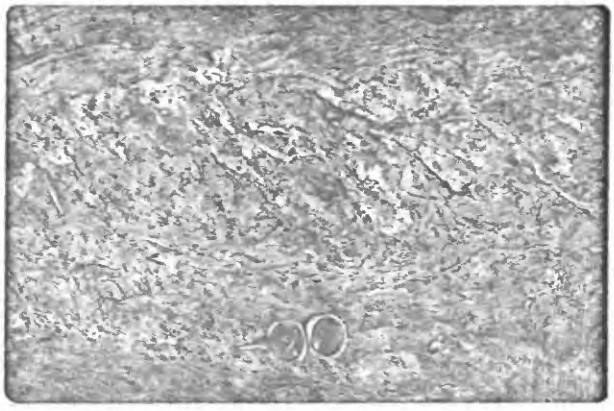

Figure 15

Primary deformation of lake sediments at the backroad pit. Brunton compass is level. Compare with deformation in figure 12, page 54.

Subaerial gravity slumping in response to postglacial stream incision is seemingly compatible with most structural elements in the readvance cut. Outward-facing slopes at the cut face west and south. Movement to the west along the north-south thrusts, and southerly dip-slip movement on the east-west thrusts are consistent with thrusting outward toward the free-faces. It can be argued that the low-angle thrusts reflect the stres field near the base, or toe, of a slump. The maximum principal stress would be subhorizontal, as shown in the stress field for the slumped section, page 50. Only the north-south thrusts,

developed in the north wall of the pit, seem to be compatible with the slump stress field and style of deformation. Imbricate faulting on the north-south thrusts is similar to F_1 faults in the slumped section, shown in figure 5, page 33. The imbricate thrusts imply slump failure in the upper portion of the deformed section. The east-west thrusts, by comparison, are distributed throughout the outcrop, indicating the north-south compressive stress acted at all levels in the deformed zone.

Ice Readvance History of Deformation. The "bulldozing" effect of the base of readvancing ice along the bottom of Lake Merrimack is believed to have imposed a subhorizontal compressive stress on the lake sediments. Initial compression folded and rotated the beds, producing the large plunging syncline. Small drag folds developed at the base of the section where the sediments retained some cohesion and folded in a ductile manner. Direction of movement on the deduced slip-line, stereogram d in figure 14, parallels the till fabric point maxima, establishing a south-southwesterly flow of the ice. The deduced direction of ice movement is also compatible with dip-slip direction of the east-west group of thrusts. Strike and dip of east-west thrusts are varied, implying rotation of the fault planes during readvance deformation. It is believed that a minor lobe of ice in the Merrimack valley extended south of the receding upland ice margin

(Koteff, 1970, personal communication). The front of the ice was probably concave southward, due to calving of the ice in the center of the lake. The edges of the ice were supported by the underlying lake bottom sediments in shallow water on either side of the valley. The glacier snout would have trended approximately east-west in the vicinity of the airport. Thus, the south-southwesterly direction of ice flow on the east side of the valley was a function of local topographic control and the orientation of the front of the readvancing ice lobe.

Some members of the tension group may be extension features related to subhorizontal compression deduced from the thrusts. Alternatively, wasting of the ice and consequent tensional release in the sediments may have produced tensional elements in the outcrop, including the sand dikes developed at the base of the till. The north-south thrusts, clearly the youngest structures in the outcrop, may be products of subsqueous slumping subsequent to ice recession. On the other hand, the north-south thrusts may have developed subaerially in response to postglacial stream cutting.

Chapter 6

QUATERNARY HISTORY

History of Study-area

Pre-Wisconsinan Deglaciation History. Tertiary erosion carved a drainage network regionally on an erosion surface of low relief (Jahns, 1953). It is believed that the Merrimack valley was well established prior to glacial advance. Multiple glaciation of the study-area may be recorded by the lower and upper tills. Depth of oxidation in the lower till is over ten feet at the two-till cut. Regionally, the depth of oxidation of the lower till is over 20 feet (Pessl and Koteff, 1970). Such deep oxidation zones indicate a long period of subaerial weathering antecedent to Wisconsinan glaciation, possibly the Sangamon interglacial stage. Pleistocene ice scour smoothed the preglacial topography and streamlined upland hills in a south-southeast direction. Ice erosion may have widened and slightly deepened the Merrimack River valley. Local striations and grooves indicate that Wisconsinan ice moved in a southerly to southeasterly direction

Recessional Ice Positions. Recessional positions of the stagnant zone and retreating solid-ice border are

deduced from outwash sequence heads, based on the sequence concept of Jahns, discussed on page 18 . Both the golf course and powerline sequences apparently mark one retreatal line of the ice about one mile above the southern map border. Each outwash channel headed against the solid-ice margin, and meltwater flowed south between stagnant blocks of ice and exposed upland slopes. A stagnant ice zone may have been one mile wide near the powerline sequence. A slightly younger stagnation zone is represented by the kame north of the golf course, and the small deposit of ice-contact gravel at the northwest end of the powerline sequence. Downwastage of the stagnant ice zone bared the Kimball Road outwash channel. Meltwaters incised the channel in till and deposited outwash sands around the golf course kame. Another retreatal line is marked by gravel outwash in the airport spillways south of Cohas Brook. Ice occupying the Cohas Brook basin impounded water against the highlands to the south. Meltwaters laid down coarse glacial debris in the spillways as the waters scoured the channels to base level -- the Lake Merrimack water plane. Further ice withdrawal opened the Cohas Brook basin to complete inundation by the lake waters. The lake extended through the passageway presently occupied by Cohas Brook. The northernmost retreatal position associated with the study-area was at the heads of the melt-

water channels north of I-93. Meltwater carried outwash sediments down these channels to the lake delta complexes in Cohas Brook basin.

The maximum extent of the readvance is unknown. It is believed that the distorted lake sediments at the readvance cut represent only a minor fluctuation of the receding ice lobe in the Merrimack valley. Ice deformation at the readvance site is older than the slump movements at either the back-road pit or slump pit. The offshore sediments at the readvance cut were apparently deposited before the offshore silts in the other pits, because the laminated lake beds in the back-road and slump pits interfinger with younger delta sands. Sand beds lie above the till at the readvance cut, and are not present in the deformed section.

Terrace and Floodplain Development. The highest terrace, traced almost continuously along the east side of the Merrimack valley, marks initial river down-cutting and lateral erosion subsequent to the lowering of the Lake Merrimack drift dam near Nashua, New Hampshire. The highest terrace is shown developed in tributary drainage paths in the Cohas Brook basin, and south of the airport in plate 1. Further erosion of the dam resulted in the cutting of lower terraces, confined to the middle of the valley, as shown in plate 1. Several of the lower terraces

are unpaired; i.e., they have no correlative surface west of the present river. A few lower levels, however do have equivalent counterparts in the western portion of the Manchester South quadrangle. Apparently, base level lowered gradually, so that lateral erosion widened some of the terrace surfaces during downcutting. In addition, large delta complexes may have established temporary local obstructions to river flow, causing lateral erosion in the valley upstream from the local barriers. Terraces in the Cohas Brook basin are graded to the local outlet just north of the airport. The base of the deep, muck-filled depression is below the 190-foot outlet, based on core depths discussed on page 16 . The basin muck apparently filled a large kettle hole, roughly outlined by the present swamp boundary.

Born and Ritter (1970, p. 1240) documented the development of six terraces along the Truckee River in western Nevada. The river cut the terraces in 44 years after extremely rapid lowering of its base level. The authors suggest that rapid draining of drift-dammed glacial lakes may be accompanied by similar terrace development. It is proposed that failure of the Lake Merrimack dam occurred in rapid downcutting stages. Terraces developed in the present study-area in response to temporary halts in downward erosion of the dam, as well as local delta obstruction to downcutting.

Archaeological sites, and associated carbon-14 dates, in north Manchester establish minimum absolute ages of terraces and the modern Merrimack River floodplain. A date of 7,650 ± 400 B.P. was obtained from remnants of a Paleo-Indian campfire on the lowest terrace above the present flood plain (Dincauze, 1971, written communication). The locality is adjacent to bedrock rapids in the river channel, and the site may have been a fishing locality where the Indians speared salmon migrating upstream to spawn (Koteff, 1970, personal communication). A fluted point was found in dune sand on a higher terrace, but it was not associated with datable material. The fluted point is indicative of a culture dated about 11,000 B.P. in other parts of New England. Based on the above ages, it is inferred that Lake Merrimack drained prior to 11,000 B.P. Regionally, ice-block collapse structures in upper terraces imply draining of the lake shortly after deglaciation of the area. However, large ice blocks buried in delta sands may have survived tens, or even hundreds of years following deglaciation. Proposed regional ice recession isochrons, shown in plate 2, indicate a maximum date of 12,800 B.P. for the draining of the lake. This date corresponds to the proposed date of deglaciation for Franklin, New Hampshire, the northern-most extent of lake sediments. The ancestral Merrimack River had established the modern floodplain level

above a bedrock channel by the eighth millenium B.P. Recent lateral erosion has widened the floodplain locally (Hitchcock and Upham, 1878).

Eolian Deposition. Large bodies of wind-blown sand accumulated on the east side of the Merrimack valley following the draining of Lake Merrimack. A sand-blasted quartz vein in the adjacent Nashua North 7.5' quadrangel indicates that the prevailing winds were northwesterly at the time of eolian activity. The prevailing winds picked up sand from the barren delta and terrace surfaces, and deposited it in thick dunes on upper terrace surfaces and on the uplands. Vegetation later stabilized the dunes, though a small dune field just north of Litchfield Road is still unprotected and active.

Regional Deglaciation History

Regional Isochrons. Inset A of plate 2 shows fairly-well established, radiocarbon-dated recessional ice margin positions in Connecticut, Massachusetts, Maine, Vermont and Quebec. Summaries of the age determinations are presented by Schafer and Hartshorn (1965), Borns (1963), and McDonald (1967). Retreatal isochrons were drawn through New Hampshire after consideration of the mode of deglaciation of the study-area, and principles of ice retreat discussed below. The siochrons show the proposed lobate nature of the ice margin during deglaciation. Deglaciation of New England was rapid:

the ice retreated 250 miles, from central Connecticut to southern Quebec, in 1,300 years. Note that the study-area was deglaciated about 13,000 years ago.

Deglaciation Model for New Hampshire

Nature of Ice Margin. Jahns (1941) emphasized the existence of a frontal ice-block stagnation zone, up to 4.5 miles wide in northeast Massachusetts, marginal to the receding "relatively solid ice" border. Was the Laurentide ice sheet active during recession of its solid-ice margin, or did it passively melt down and back to the north? The best evidence for actice ice retreat are exposures that show till overlying disturbed outwash or lake sediments. The ice sheet must have readvanced over its own debris at such localities. Several such readvance sites are described by Upham (1878, p. 131-136). Antevs (1922, p. 81-82), and J. W. Goldthwait (1951, p.47). The readvance localities are shown in plate 2, south of the White Mountains, and in the Connecticut River valley. The location of the readvance cut described in chapter 5 of this report is shown in south-central New Hampshire. In these areas, normal gravitational outflow of Laurentide ice was continuous as the ice margin melted back. By remaining internally active during recession, the ice sheet maintained a thinned, but relatively solid front behind the stagnation zone.

Theoretical Glacier Gradient. Nye (1952, p. 92) calculated that the profile of an ideal circular ice-cap, taken along a direction of flow, would be $h = 4.8\sqrt{d}$, where h (meters) is the thickness of the glacier at a point d (meters) distance from the glacier terminus. Hollin (1962, p. 178) discovered that the cross-profile within 235 miles of the terminus of the Antarctic ice sheet is defined by the equation $h = 4.7\sqrt{d}$. Topographic highs below the ice apparently have little effect on the glacier gradient (Robin, 1962, p. 141). Nye's equation for the surface gradient of a plastically flowing ice-cap was used in the construction of the ice shadow in New Hampshire, shown in plate 2.

Obstacles to Glacier Flow. Prominent topographic features may intercept the glacier surface during ice retreat. Figure 16 show two ice sheet positions: the dashed line represents the surface gradient of the ice sheet before the mountain mass intercepts the glacier surface. The solid line shows the furthest extent of the glacier snout at the instant of nunatak emergence. Provided no extreme flow of ice takes place through adjacent cols, the mass of ice in front of the nunatak is cut off from the active ice sheet. The stranded ice forms a wide stagnation zone in the ice shadow of the mountain barrier.

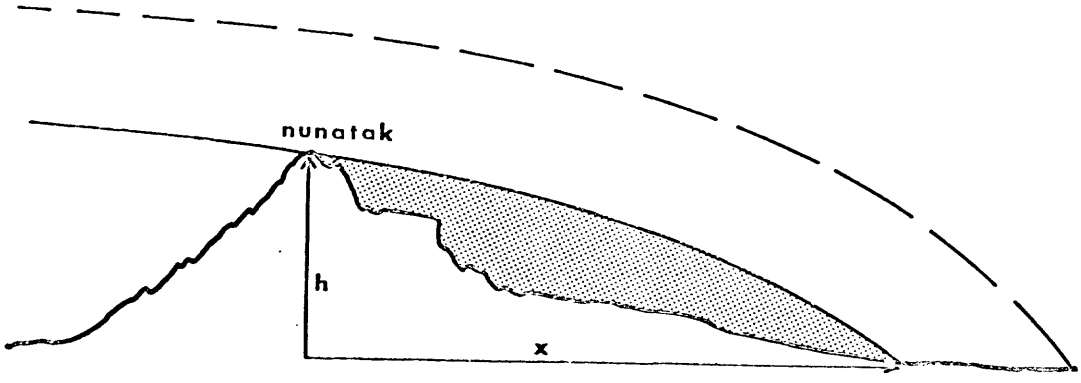

Figure 16

Barrier to glacier flow. h(meters) is the thickness of the glacier at d(meters) distance from the glacier terminus. The curve of the glacier surface is defined theoretically by Nye (1952, p. 92). The stippled area below the solid line is the stranded ice block.

Borns (1970) has argued that a mountain barrier interfered with normal glacier outflow during recession of the ice-sheet in Maine. Eskers are traced continuously up to fifty miles in Central Maine, indicating that a large ice shadow existed south of the Appalachians of northern Maine. J. W. Goldthwait (1951, p. 14) pointed out the mountain barrier to glacier flow in New Hampshire.

Ice Shadows in New Hampshire. Plate 2 shows present 1000-foot contours of New Hampshire depressed at the rate of five feet per mile along a northwest-southeast trending line. The line of depression (from Flint, 1957, p. 251) is assumed to be the line of the maximum postglacial isostatic upwarp gradient. The readvance locality described in this

report was arbitrarily chosen as the point of no depression. The calculated downwarp effectively reduces mountain peaks to Wisconsinan glacial stage elevations, relative to other peaks. Absolute elevations could be calculated for each contour line if the position of the New England hingeline was known (see Flint, 1957, p. 254). Striation directions were taken from J. W. Goldthwait (1922; in Flint, 1957, p. 60).

The dotted line south of the White Mountains represents the southern boundary of a Wisconsinan ice shadow in central New Hampshire. The ice shadow was constructed on a nearly north-south ice flow direction that parallels the striae orientations on the mountain tops. The southern limit of the ice shadow was determined by the intersection of the depressed mountain peaks with the theoretical glacier surface gradient, as shown in figure 16. The longest portion of the ice shadow extends south of Mt. Washington into the Lake Winnipesaukee region. Portions of the outlined ice shadow may correspond to the large stagnant ice zone proposed by J. W. Goldthwait (1938). Note, however, that striae directions trend southeasterly south of the mountains, implying that the outlined north-south ice shadow is inconsistent with direction of ice flow.

It is suggested that striation orientations represent the direction of ice movement during the latter phases of glaciation, possibly movement during the deglaciation phase.

Older striae, carved at the beginning of the glacial stage, were eroded by subsequent ice scour. Striae in northern New Hampshire are generally younger than striae in the south-central part of the state, if the above assumption is true. Likewise, the north-south striae on top of the White Mountains reflect the direction of ice flow there just before nunatak emergence. It is proposed that the southeasterly striae, extensively developed in south-central New Hampshire, are younger than the north-south striae on top of the mountains. The southeasterly striae, therefore, record the movement of a late-Wisconsinan ice lobe that flowed around the White Mountain nunataks, into the Lake Winnipesaukee region. No major mountain barriers existed in the west-central part of New Hampshire, as shown by the depressed contours in plate 2. The ice sheet flowed relatively unimpeded across the central part of the state. The true ice shadow for the White Mountains extended southeast from the barrier into Maine. The shadow is not shown in plate 2. Lobate retreatal isochrons, however, reflect the orientation of the ice shadow in inset A of plate 2.

North-south striae are predominent in northern Massachusetts. These striae may be the same age as the north-south striae carved on the tops of the White Mountains prior to nunatak emergence. If this assumption is correct, the regional ice flow direction could have been

north-south when the ice sheet terminus lay south of Massachusetts. In other words, at the maximum glacial phase, ice flow was relatively unaffected by the White Mountain barrier. During ice recession, and consequent thinning, the mountain barriers gradually influenced glacier flow until a major diversion developed west of the White Mountains. The flow diversion probably occurred prior to nunatak emergence. For instance, southeast striae in southern New Hampshire show that ice flow was predominantly southeasterly when the ice margin stood at the Massachusetts-New Hampshire border. Ice thickness over Mt. Washington is calculated to be 1700 feet at this time, according to Nye's theoretical model.

The proposed regional isochrons, shown in inset A of plate 2, indicate the southeasterly movement of the ice lobe that flowed around the White Mountains. Emergence of the White Mountain nunataks occurred about 12,900 B.P., because the proposed 12,900 terminal isochron in western Maine lies within the calculated ice shadow of Mt. Washington. Small ice shadows, stippled in plate 2, were constructed along southeasterly flow lines parallel to local striation directions. The small ice shadows probably contained large stagnant ice blocks following deglaciation of each area. The Lake Winnipesaukee readvance sites indicate that the margin of the receding Laurentice ice lobe remained active

during northwesterly retreat. It is believed that these readvance sites represent only minor ice marginal fluctuations, and not a single large readvance of the Winnipesaukee lobe. The lobate form of the isochrons in plate 2 emphasizes the effect of local topography on the active ice margin. Tongues of ice extend into valleys, and areas of high relief form reentrants along the ice border. Regional correlations in Maine and Vermont are not clear. Note, however, that the margin of the Connecticut Valley lobe, represented by the 12,750 isochron, corresponds with the position of the Danville moraine in eastern Vermont, discussed by Stewart and MacClintock (1969, p. 81). Local striation and till fabric orientations near the Danville moraine (Stewart, et. al., 1970) indicate a southwesterly flow of ice at the western edge of the Connecticut valley ice lobe.

In their isochronal maps, Prest (1968, 1970) and Bryson, et al. (1970) show closed isochrons around the Green Mountains, White Mountains, and mountains in northern Maine. The closed isochrons imply the existence of late-Wisconsinan ice caps, or large valley glaciers in the uplands of New England. No closed isochrons appear in plate 2. Instead, large ruled areas are shown in the White Mountains. These areas represent stranded Laurentide ice blocks that remained in deep valleys following emergence

of the nunataks. These ice blocks may have acted as nuclei for local valley glaciers in late-Wisconsinan time.

Chapter 7

CONCLUSIONS

Major conclusions from this study are:

(1) Till stratigraphy in the study-area confirms others' observations that the upper and lower tills represent two ice advances in New England. The unique two-till cut on Mammoth Road clearly shows two distinct facies of the upper till: lodgement and ablation. The lower till is not the basal unit of the upper till, deposited by Wisconsinan ice. Depth of oxidation in the lower till indicates a long period of subaerial weathering. The lower till may represent a pre-classical Wisconsin (Altonian ?) ice advance before 25,000 B.P. The lower till may, however, represent an Illinoian ice advance in New England.

(2) Outwash sequences mark retreatal ice margin positions in the study-area. The sequences are similar to those described by Jahns in northern Massachusetts, and sequences mapped by Koteff in southern New Hampshire. Younger sequences abut ice-contact deposits, indicating an orderly, northward retreat of the ice margin. A stagnation zone existed in front of the receding ice margin. The stagnation zone may have been one mile wide near the southern border of the study-area.

(3) Pore-water pressure in sandy lake sediments at the slump pit increased as lake sedimentation continued. Slump movement occurred as normal stresses acting on the plane of failure were reduced to very low values. The direction of slip of each fold generation is parallel to slip-lines deduced from rotation senses of the drag folds.

(4) The deduced drag fold slip-line at the re-advance cut is parallel to the point maxima of the till fabrics and dip-slip direction on one group of faults. Ice movement was south-southwesterly. Younger faults mark post-readvance release and slump slip.

(5) The retreating Laurentice ice sheet had an active margin behind the stagnation zone.

(6) The White Mountains apparently acted as a barrier to ice movement during deglaciation of New Hampshire. The base of the ice sheet had begun to flow around the mountain barrier when the active ice margin had retreated to the latitude of the study-area.

BIBLIOGRAPHY

Antevs, Ernst, 1922: The Recession of the Last Ice Sheet in New England; Am. Geog. Soc., Res. Ser. No. 11.

Billings, M. P. 1954; Structural Geology; Prentice-Hall, 514 pp.

Born, Stephen M., and Ritter, Dale F., 1970: Modern Terrace Development Near Pyramid Lake, Nevada, and Its Geologic Implications; Bull. Geol. Soc. Amer., v. 81, pp. 1233-1242.

Borns, Harold W., and Calkin, Parker E., 1970: Quaternary History of Northwestern Maine; in Guidebook for N. E. I. G. C. Field Conf., pp. E-2m 1-6.

Bryson, R. A., et. al., 1969: Radiocarbon Isochrones on the Disintegration of the Laurentice Ice Sheet; Arc. and Alp. Res., v. 1, pp. 1-14.

Denny, C. S., 1958: Surficial Geology of the Canaan Area, New Hampshire; U. S. Geol. Sur. Bull. 1061-C, 101 pp.

Flint, R. F., 1957: Glacial and Pleistocene Geology; John Wiley and Sons, 553 pp.

Glen, J. W., Donner, J. J., and West, R. G., 1957: On the Mechanism by which Stones in Till Become Oriented; Am. J. Sci., v. 255, pp. 194-205.

Goldthwait, J. W., 1938: The Uncovering of New Hampshire by the Last Ice Sheet; Am. J. Sci., v. 36, pp. 345-372.

Goldthwait, J. W., Goldthwait, G. L., and Goldthwait, R. P., 1951: The Geology of New Hampshire, Part 1 - Surficial Geology; N. H. St. Planning and Devel. Comm., 83 pp.

Green A. R., 1964: Magnitude and Frequency of Floods in the United States, Part 1-A, New England; U. S. Geol. Sur. Water Supply Paper 1671.

Handin, J., et al., 1963: Experimental Deformation of Sedimentary Rocks Under Confining Pressure: Pore Pressure Tests; Bull. Amer. Assoc. Pet. Geol. v. 47, pp. 717-755.

Hansen, Edward, et al., 1961: Décollement Structures in Glacial-Lake Sediments; Bull. Geol. Soc. Amer., v. 72, pp. 1415-1418.

Hansen, Edward, 1965: Methods of Deducing Slip-Line Orientations from the Geometry of Folds; in Ann. Rep. of the Carnegie Geophys. Lab., pp. 387-405.

Hartshorn, J. H., 1958: Flowtill in Southeastern Massachusetts; Bull. Geol. Soc. Ameri., v. 69, pp. 477-481.

Hitchcock, C. H. (and Upham, W.), 1878: Surface Geology in The Geology of New Hampshire, Part III, St. Printer, pp. 3-340.

Hollin, J. T., 1962: On the Glacial History of Antartica; J. Glaciol., v. 4, pp. 173-195.

Holmes, C. D., 1941: Till Fabric; Bull. Geol. Soc. Amer., v. 52, pp. 1301-1354.

Hubbert, M. K., 1951: Mechanical Basis for Certain Familiar Geologic Structures; Bull. Geol. Soc. Amer., v. 62, pp. 355-372.

Hubbert, M. K., and Rubey, W. W., 1959: Mechanics of Fluid-filled Porous Solids and its Application to Overthrust Faulting; Bull. Geol. Soc. Amer., v. 70, pp. 115-166.

Jahns, R. H., 1941: Outwash Chronology in Northeastern Massachusetts [abs.] ; Bull. Geol. Soc. Amer., v. 52, p. 1910.

Jahns, R. H., 1953: Surficial Geology of the Ayer Quadrangle, Massachusetts; U. S. Geol. Sur. Geol. Quad. Map GQ-21.

Koteff, Carl, 1970: Surficial Geologic Map of the Milford Quadrangle, Hillsborough County, New Hampshire; U. S. Geol. Sur. Geol. Quad. Map GQ-881.

McDonald, B. C., 1967: Pleistocene Events and Chronology in the Appalachian Region of Southeastern Quebec, Canada; Ph.D. Dissert., Yale Univ., 161 pp.

Munsell Soil Color Charts, 1954, Munsell Color Co., Inc., Baltimore, Md.

Nye, J. F., 1952: The Mechanics of Glacier Flow; J. Glaciol. v. 2, pp. 82-93.

Pessl, Fred Jr., and Koteff, Carl, 1970: Glacial and Postglacial Stratigraphy along Nash Stream, northern New Hampshire; in Guidebook for N.E.I.G.C. Field Conf., pp. G, 1-15.

Pessl, Fred, Jr., and Schafer, J. P., 1968: Two-till Problem in Naugatuck-Torrington Area, Western Connecticut; in Guidebook No. 2, N.E.I.G.C. Field Conf., pp. B-1, 1-25.

Prest, V. K., 1969: Retreat of Wisconsin and Recent Ice in North America; Geol. Sur. Can. Map 1257A.

_____, 1970: Quaternary Geology of Canada, in Econ. Geol. Report No. 1, Dept. of Energy, Mines and Resources, Ottawa, Can., pp. 676-764.

Ragan, D. M., 1968: Structural Geology, an Introduction to Geometrical Techniques: John Wiley and Sons, 166 pp.

Ramsay, J. G., 1967: Folding and Fracturing of Rocks; McGraw-Hill, 568 pp.

Robin, G. deQ., 1962: The Ice of the Antartic; Scient. Amer., v. 207, pp. 132-146.

Sanford, A. R., 1952: Analytical and Experimental Study of Simple Geologic Structures; Ball. Amer. Assoc. Pet. Geol., v. 70, pp. 19-52.

Schafer, J. P., and Hartshorn, J. H., 1965: The Quaternary of New England; in Wright, H. E.; and Frey, D. G., The Quaternary of the United States; Princeton Uni . Press, pp. 113-118.

Scott, W. H., 1969: Experiments in Flow Deformation. in Ann. Rep. of the Carnegie Geophys. Lab., pp. 251-258.

Simmons, C. S., et al., 1953: Soil Survey of Hillsborough County, New Hampshire; U. S. Dept. Agr., Soil Cons. Ser.

Sriramada, Aluru, 1966: Geology of the Manchester Quadrangle, New Hampshire; N. H. Dpet. Res. and Econ. Devel., Bull. 2, 78 pp.

Stewart, D. P., and MacClintock, P., 1969: The Surficial Geology and Pleistocene History of Vermont; Dept. Water Res., Bull. No. 31, 251. pp.

Stewart, D. P., et al. 1970: Surficial Geologic Map of Vermont.